

**UCLA**

**UCLA Electronic Theses and Dissertations**

**Title**

Aircraft Operations and Their Influence on UFP Concentrations In Communities Surrounding Two Airports

**Permalink**

<https://escholarship.org/uc/item/68q348w6>

**Author**

Alvarado, Erica Leah

**Publication Date**

2018

Peer reviewed|Thesis/dissertation

UNIVERSITY OF CALIFORNIA

Los Angeles

Aircraft Operations and Their Influence on UFP Concentrations  
In Communities Surrounding Two Airports

A dissertation submitted in partial satisfaction of the  
requirements for the degree Doctor of Environmental Science and  
Engineering

by

Erica Leah Alvarado

2018



## ABSTRACT OF THE DISSERTATION

### Aircraft Operations and Their Influence on UFP Concentrations In Communities Surrounding Two Airports

by

Erica Leah Alvarado

Doctor of Environmental Science and Engineering

University of California, Los Angeles, 2018

Professor Suzanne E. Paulson, Chair

Emissions from aircraft operations can substantially increase concentrations of several pollutants in communities near airports, especially ultrafine particles (UFP), which have also been suggested to impact air quality up to several kilometers (km) downwind. Aircraft engines are tested for emissions of several pollutants, but none of the tests are specifically aimed at UFP. Here, data from two airports, Santa Monica Airport (SMO) and Los Angeles Insertional Airport (LAX) were analyzed to determine aircraft contribution to UFP concentrations at sites downwind of the two airports, respectively. At SMO, peak UFP concentrations associated with individual takeoff and landing operations were analyzed. A single variable linear regression was run separately for aircraft engine emission rates and takeoff and landing UFP peak concentrations to determine which, if any, parameters are predictive for UFP. Parameters included nitrogen oxides [NO<sub>x</sub>],

carbon monoxide [CO], hydrocarbons [HC], smoke number [SN], and engine thrust identified in the International Civil Aviation Organization (ICAO) database. Data from the Los Angeles World Airports Air Quality and Source Apportionment Study were analyzed for relationships between particle concentration and wind direction, time of data, and aircraft. Additionally, contribution from arrival and departures by runway (24 and 25), arrivals compared to departures, and diurnal UFP concentrations is determined.

For SMO, we were able to assign specific peak UFP concentrations for both takeoff and landing operations with takeoff peaks significantly higher than landing. Using single variable linear regressions analysis showed using ICAO database parameters to predict UFP peak measurements is best made by using thrust (kN) and  $\text{NO}_x$ . For LAX, multiple lines of evidence indicate aircraft landing operations are the primary contributor to UFP concentrations  $< 30$  nm at two sites between 1,600 and 2,000 m downwind of LAX. Sub-30 nm UFP are highly elevated when the sites are downwind of arrival operations on one or both runways. Of the aircraft operation influence at the two sites, UFP concentrations  $< 30$  nm are found to be primarily from arrivals on Runways 24 and 25. For the multivariate linear regression results, arrivals were significant when the two sites were downwind of the airport while departures were not.

The dissertation of Erica Leah Alvarado is approved.

Irwin H Suffet

Yifang Zhu

Michael Leo Brenna Jerrett

Suzanne E. Paulson, Committee Chair

University of California, Los Angeles

2018

## Table of Contents

Introduction.....	1
Literature Review of Aircraft Emissions and a Comparison of Emission Rates from the International Civil Aviation Organization (ICAO) Database and Field Studies .....	3
Introduction.....	3
Aircraft Engine Emissions .....	4
Aircraft Particulate Emissions.....	6
UFP Measurements Downwind of Airport .....	8
Aircraft Mode Contributions.....	8
International Civil Aviation Organization Measurements and Requirements .....	10
Comparison of ICAO Emissions and Field Measured Values.....	12
UFP, Health, and ICAO Database Parameters.....	13
References .....	15
Use of International Civil Aviation Organization Database Parameters to Determine UFP Concentrations at Santa Monica Airport.....	22
Abstract .....	22
1. Introduction .....	24
2. Methods.....	26
2.1 Sites .....	26
2.2 SMO Operations.....	28
3. Results and Discussion .....	29
3.1 Takeoff versus Landing.....	29
3.2 Difference between Sites .....	31
3.3 ICAO Parameters and Operations .....	32
3.4 Engine Age .....	36
4. Conclusions and Recommendations .....	38
Appendix.....	40
References .....	44
Impact of Los Angeles International Airport on UFP Concentrations at Two Downwind Sites: Analysis Using Wind Direction, Diurnal Patterns, and Operational Composition.....	50
Abstract .....	50
1. Introduction .....	51

2. Methods.....	53
2.1 Sites .....	53
2.2 Data Set.....	54
2.3 LAX Operations .....	57
3. Results and Discussion.....	57
3.1 General Features of UFP at the CE and CN Sites .....	57
3.2 Multivariate linear regression.....	65
4. Discussion.....	69
Appendix .....	72
References .....	78
Conclusion .....	84
References .....	88



## List of Figures

### Chapter 2: SMO

Figure 1: Study area for SCAQMD Supplemental Study.....	27
Figure 2: UFP concentrations $\pm$ 5 minutes from a sample takeoff event.....	30
Figure 3: UFP concentrations $\pm$ 5 minutes from a sample takeoff event.....	30
Figure 4: Thrust (kN) and UFP peak concentrations at the Ernst Site for takeoff operations .....	34
Figure 5: NO <sub>x</sub> emission rates for LTO cycle and UFP peak concentrations at the Ernst Site for takeoff operations.....	35
Figure 6: UFP peak concentrations compared to engine age for departures at RW site.....	37
Figure 7: UFP peak concentrations compared to engine age for departures at Ernst site.....	38

### Chapter 2 Appendix

Figure A1: UFP peak concentrations for arrival operations per aircraft.....	42
Figure A2: Scatterplots and correlation matrix for correlations between NO <sub>x</sub> , HC, CO, SN, and thrust for takeoff emissions rates for takeoff operations.....	43

### Chapter 3: LAX

Figure 1: LAX AQSAS site locations.....	55
Figure 2: Wind rose plot for Summer Season at the Community East site.....	56
Figure 3a: Particle number size distribution for CE site for wind directions placing site downwind at 225-315° and wind directions placing site upwind at 45-135°.....	59
Figure 3b: Particle number size distribution for CN site for wind directions placing site downwind at 225-315° and wind directions placing site upwind at 45-135°.....	59
Figure 4a: Diurnal half-hour averages for the entire study season for UFP concentrations < 30 and 30 – 98 nm at the CE and CN sites for RW24/25.....	61
Figure 4b: Arrivals operational counts by runway and average wind speed.....	62
Figure 4c: Total vehicles per hour for 7/18-8/28/2012 and total departures operational counts by runway.....	62
Figure 5a: Polar plots of UFP concentrations at the CE site for < 30 nm.....	64
Figure 5b: Polar plots of UFP concentrations at the CN site for < 30 nm.....	64
Figure 5c: Polar plots of UFP concentrations for the CE site for 30-98 nm.....	64
Figure 5d: Polar plots of UFP concentrations for the CN site for 30-98 nm.....	64
Figure 6: Actual versus predicted UFP concentration (< 30 nm) for multivariate regression results at the CE site for wind directions 285-345°.....	67

Figure 7: Actual versus predicted UFP concentration (< 30 nm) for multivariate regression results at the CN site for wind directions 285-345° .....	69
---	----

Chapter 3 Appendix

Figure A1: Actual versus predicted UFP concentration (< 30 nm) for multivariate regression results at the CE site for wind directions 45-105° .....	74
Figure A2: Actual versus predicted UFP concentration (< 30 nm) for multivariate regression results at the CE site for wind directions 105-165° .....	74
Figure A3. Actual versus predicted UFP concentration (< 30 nm) for multivariate regression results at the CE site for wind directions 165-225° .....	75
Figure A4. Actual versus predicted UFP concentration (< 30 nm) for multivariate regression results at the CE site for wind directions 225-285° .....	75
Figure A5. Actual versus predicted UFP concentration (< 30 nm) for multivariate regression results at the CN site for wind directions 45-105° .....	76
Figure A6. Actual versus predicted UFP concentration (< 30 nm) for multivariate regression results at the CN site for wind directions 105-165° .....	76
Figure A7. Actual versus predicted UFP concentration (< 30 nm) for multivariate regression results at the CN site for wind directions 165-225° .....	77
Figure A8. Actual versus predicted UFP concentration (< 30 nm) for multivariate regression results at the CN site for wind directions 225-285° .....	77

**List of Tables**

Chapter 2: SMO

Table 1: Data Set Utilized for Study .....	29
Table 2: Average UFP Peak Concentration by Site .....	31
Table 3: Linear Regression Coefficients and P-Values for ICAO Emission Rates and UFP peak Concentrations .....	33

Chapter 2 Appendix

Table A1: Average UFP Measurements Before, During, and After Repaving Project .....	40
Table A2: Range in UFP Peak Concentration for Arrivals and Departures by Aircraft .....	41

Chapter 3: LAX

Table 1: Regression Coefficients and p-values for CE Site UFP Concentrations < 30 nm .....	66
Table 2: Regression Coefficients and p-values for CN Site UFP Concentrations < 30 nm .....	68

Chapter 3 Appendix

Table A1: Operations by Runway .....	73
--------------------------------------	----

## **Vita/Biographical Sketch**

Erica Leah Alvarado, M.P.H.

### **Education**

B.A., Biology with Marine Science Concentration, Boston University, Boston, MA 2005  
M.P.H., Environmental Health Science, University of California Los Angeles, 2009

### Registrations/Certifications

Accredited California Air Resource Board Greenhouse Gas Emission Verifier, Executive Order H-15-004

### **Employment**

Tetra Tech, Inc.

Environmental Scientist

- Carried out research for the Los Angeles World Airport Air Quality and Source Apportionment Study
- Conducted greenhouse gas verification services as a California Air Resources Board-certified Greenhouse Gas Lead Verifier with specialties in oil and gas, transactions, and process emissions sources
- Prepared emission reduction totals for the New York City Department of Transportation Hunts Point Clean Trucks Program

California State University

Northridge, Lecturer

- Instructor for Interdisciplinary Perspectives on Sustainability for Spring 2016 for a class of 49 students
- Covered topics including: climate change, urban planning, environmental policy, sustainability and health, environmental justice, business and sustainability, ecosystems, fossil fuels and pollution, and water and pollution

University of California, Los Angeles

Graduate Student Researcher

- Carried out team research related to odor problems in drinking water to determine where the public will identify and object to particular odors

Los Angeles County Department of Public Health

Graduate Student Researcher

- Carried out individual and team research related to environmental health policies, exposure and risk assessments, and active living and healthy community policies involved Los Angeles area health issues
- Provided input on the inclusion of health-related language in community planning documents

## **Introduction**

Aircraft are a large source of pollutants, including carbon monoxide (CO), black carbon (BC), oxides of nitrogen (NO<sub>x</sub>), sulfur dioxide (SO<sub>2</sub>), partially combusted or unburned hydrocarbons (HC), black carbon (BC), particulate matter, including ultrafine particles (UFP), and other trace elements. Concentrations of several of these, especially UFP and BC, can increase concentrations in communities near airports as well as up to several kilometers (km) downwind. Many studies report that exposure to increased concentrations of UFP can be linked to increased risk of cardiovascular disease and detrimental effects on pulmonary functioning.

The overall objective of this study is to analyze UFP concentrations from aircraft at multiple community sites located downwind of two airports, Santa Monica Airport (SMO) and Los Angeles International Airport (LAX). Specific objectives differ for each airport depending on data composition and site location.

At SMO, UFP measurements collected at two community sites, located 35 and 100 meters (m) downwind of the end of the runway, are analyzed for the ability to associate takeoff and landing UFP peak concentrations to specific aircraft events. Additionally, characteristics of UFP from takeoff compared to landing are explored. While the literature does include studies where UFP peak concentrations were associated with individual takeoff operations, few, if any, studies reported UFP peak concentrations associated with landing events.

Aircraft engines are required to be tested for several pollutants, including NO<sub>x</sub>, HC, CO, and smoke number (SN), and reported to the International Civil Aviation Organization (ICAO) for inclusion in the database. However, none of the tests are specifically aimed at UFP. Here, the ability of ICAO database parameters is explored to determine which, if any, parameters are able to predict UFP concentrations from aircraft.

The literature contains few studies focusing on engine age and differences in UFP concentrations. Aircraft engines, vintage, and associated UFP concentrations are analyzed for differences between “older” versus “newer” engines to determine dependence of UFP concentrations on engine vintage.

At LAX, UFP measurements were taken at two community sites located 1,600 and 2,000 m downwind of the end of the North and South Airfields, respectively. Analysis of the data included the ability to determine contribution of aircraft takeoff and landing operations to UFP measurements at the two sites. Additionally, UFP concentrations from arrivals and departures are explored to determine contributions by type of operation. There are four primary runways, located on two main airfields, at LAX with the number of arrivals and departures differing between them. The impacts from aircraft arrivals and departures by runway are analyzed for overall contribution by operation to UFP concentrations at the two community sites.

The dependence of two UFP particle size bins,  $< 30$  nm and  $30 - 98$  nm, on wind direction and time of day are analyzed. This is to determine impact of the airport, specifically aircraft operations, at the two sites, as the  $< 30$  nm particles have been reported in the literature to result primarily from aircraft operations, while the  $30 - 98$  nm particles are predominantly from other sources, such as roadways. Analysis of emissions by wind direction and time of day is used to determine when the airport has the largest influence at the two sites.

# **Literature Review of Aircraft Emissions and a Comparison of Emission Rates from the International Civil Aviation Organization (ICAO) Database and Field Studies**

## **Introduction**

Airports are a source of multiple types of emissions contributing to pollution in surrounding areas, including many local communities. Approximately 10 percent of aircraft pollutant emissions and 30 percent of hydrocarbon (HC) and carbon monoxide (CO) happen at less than 3,000 feet (FAA, 2015). Emission sources include, but are not limited to, aircraft, jet fuel, refueling, ground support equipment (GSE), auxiliary power units (APUs), traffic to and from the airport, and power usage at the airport. The largest source of emissions include aircraft in all operation modes, including take-off, landing, taxiing, and idling, collectively known as landing-takeoff cycle (LTO). Emissions are also measured in aircraft exhaust at cruising altitudes (greater than 3000 feet). LTO cycle modes are focused on here to determine how aircraft emissions disperse within the atmosphere and neighboring communities.

Emission types from aircraft exhaust include: carbon monoxide (CO), black carbon (BC), oxides of nitrogen (NO<sub>x</sub>), sulfur dioxide (SO<sub>2</sub>), partially combusted or unburned hydrocarbons (HC), particulate matter, including ultrafine particles (UFP), and other trace elements. While less than 1 percent of aircraft exhaust is composed of the aforementioned pollutants (FAA, 2015), these pollutants are found in areas surrounding airports and in downwind neighborhoods. Understanding the contribution of UFP emissions from airports, specifically aircraft operations, is important in determining the health impacts from such operations.

## **Aircraft Engine Emissions**

Airports are significant sources of  $\text{NO}_x$ , CO,  $\text{SO}_2$ , BC, and particulates, including particulate matter 2.5 micrometers and less in diameter ( $\text{PM}_{2.5}$ ) and UFP. These emissions primarily result from the complete and incomplete combustion of aircraft fuels. Aircraft fuels include gasoline (AVGAS) for reciprocating or piston engines and jet fuel or kerosene (Jet-A, Jet A-1, or Jet B) for turbine engines. Jet fuel has a higher carbon content than AVGAS, with the kerosene carbon content ranging from  $\text{C}_{10}$  and  $\text{C}_{16}$  (FAA, 2012), a higher viscosity, lower volatility, and higher boiling point. The sulfur content of jet fuel is also higher than gasoline. AVGAS is often comprised of HCs of varying boiling points and volatility; however, it has a low flash point, is very flammable, and overall is highly volatile (FAA, 2012). AVGAS is most commonly single 100 octane low level (100LL) with the lead content (of tetraethyl lead [TEL]) of 2 milliliters of TEL per gallon (FAA, 2012). The composition of emissions can vary depending upon the engine and its fuel type.

$\text{NO}_x$  is emitted from aircraft exhaust when small amounts of nitrogen from the surrounding atmosphere form nitrous oxides. GSE are large emitters of  $\text{NO}_x$  (Yu et al., 2004; Schurmann et al., 2007). Carslaw et al. (2006) reported  $\text{NO}_x$  emissions from Heathrow airport contribute 28 percent of annual mean  $\text{NO}_x$  and  $\text{NO}_2$  at the airport boundary with aircraft emissions observed up to 2.7 kilometers (km) downwind. While GSE are large contributors of  $\text{NO}_x$  emissions, Mazaheri et al. (2011) reported that landing/take-off (LTO) procedures of aircraft contributed 97 percent of annual overall emissions from Brisbane Airport when compared to ground running procedures.

Composition and amount of emissions from aircraft depend on the aircrafts' mode and type of fuel while the composition of HC emissions depend on an aircraft's operating mode. HC emissions are at higher levels when an aircraft is at idle (Agrawal et al., 2008; Herndon et al., 2008; Herndon

et al., 2009). Schurmann et al. (2007) reported that during taxiing, when the engine is operating at a higher temperature, the cracking of higher aromatics lead to fewer of these species but an increasing amount of benzene. Additionally, non-methane HC's contribute more significantly to particulate mass when a fuel's sulfur content goes to zero (Brock et al., 2000).

Sulfur from airport operations is primarily attributed to aircraft exhaust and is present in aviation fuel at approximately 550 to 750 parts per million (ppm) (Kapadia et al., 2015). Sulfur from aviation fuels is emitted via plane exhaust in the form of SO<sub>2</sub> and can form sulfuric acid (IPCC, 1999). SO<sub>2</sub> emissions depend on the sulfur levels in the fuel used as well as overall fuel burn (Ratliff et al., 2009). Yu et al. (2004) found SO<sub>2</sub> from Los Angeles International Airport (LAX) operations contributed approximately 1 percent of the South Coast Air Basin's SO<sub>2</sub> emissions.

Black carbon (BC) emissions from aircraft have been measured in airport adjacent communities. Higher thrust conditions result in the highest BC emission indices (Kinsey et al., 2011). Dodson et al. (2009) reported BC concentrations are positively associated with departures and arrivals, with departures having a stronger impact than arrivals. Patterns in BC concentrations were also found to be more similar to NO<sub>x</sub> measurements than particle number measurements (Klapmeyer and Marr, 2012).

Concentrations of CO measured near airport terminals were found to be dependent upon aircraft operation mode (Schurmann et al., 2007), such as taxi or idle. This corresponds to higher CO emissions for lower thrust settings, such as taxi and idle, due to incomplete fuel combustion (Schurmann et al., 2007). Taxi and idle modes are often at lower efficiency and thrust. Incomplete combustion during these operating modes results in the increased formation of CO. In the presence



of an insufficient quantity of air or fuel mixing in air in the combustion zone, there is an increase in CO emissions.

### **Aircraft Particulate Emissions**

Particulates from jet exhaust contain numerous components. The chemical composition of aircraft particulate exhaust depends on exhaust gas temperature (Onasch et al., 2009). Composition of emissions from different aircraft operational modes (idling, takeoff, landing, and climb out – for the purposes of this literature review) vary in temperature and type of particulates in aircraft exhaust. Particulate composition can also be influenced by the engine type, age, and fuel type.

Kinsey et al. (2010) observed that between 40 to 80 percent of total PM mass measured 30 m behind an aircraft engine was comprised of volatile matter (sulfur and organics). Additionally, Kinsey et al (2010) determined that emissions index versus fuel flow values were highest at idling, decreased at the mid-range power, and increased again at higher engine power. The amount of volatile matter emissions produced also depend on the engine type. Total elemental emissions from externally mixed flow CFM56 engines were generally similar; however, higher emissions were produced by internally mixed flow AE3007A1E and RB211-5354-B engines (Kinsey et al., 2010). Elemental carbon is also dependent upon engine technology. Agrawal et al. (2008) found PM composition to shift from higher organic carbon (OC) during idle to higher elemental carbon (EC) with an increase in engine power, due to fuel combustion with increasing temperature.

The peak median/mean of UFP size distribution from aircraft measurements in community settings consistently falls between 10-15 nm (Westerdahl et al., 2008; Hu et al., 2009; Zhu et al., 2011; Lobo et al., 2012; Keuken et al., 2015). UFP have been measured downwind of the airport as well as directly behind an aircraft's takeoff location. As particulates age, then tend to combine with addition materials to form secondary particulates. Emission measurements vary with, but are

not limited to, weather, wind speed, time of year, and time of day. Measurements of UFP made by Zhu et al. (2011) at LAX behind the blast fence differed slightly between summer and winter, with an average UFP sizes of 14 nm and 16.3 nm, respectively.

Takeoff and landing schedules affect concentrations of UFP. Spikes in UFP number concentrations have been found to correlate to takeoff operations (Westerdahl et al., 2008; Hu et al., 2009; Zhu et al., 2011; Keuken et al., 2015). Takeoff operations often start early in the morning and increase throughout the day, which can cause diurnal variations of UFP concentrations. Wind speed can also affect UFP measurements via mixing and transport of emissions to a receptor site. For example, LAX has a strong on-shore flow beginning mid- to late-morning and continuing throughout the day. This on-shore flow is when most takeoffs and landings happen.

While many field studies measure UFP concentrations from takeoff operations (Westerdahl et al., 2008; Hu et al., 2009; Zhu et al., 2011; Lobo et al., 2012; Choi et al., 2013; Moore et al., 2017), a number of studies have found evidence for landing operations on UFP concentrations downwind of airports (Westerdahl et al., 2008; Hudda et al., 2014; Keuken et al., 2015; Hudda and Fruin, 2016; Riley et al., 2016). Hudda and Fruin (2016) measured spikes of UFP up to 2.75 km from the airport (LAX) from landing operations. Additionally, the Hudda and Fruin (2016) observed smaller UFP sizes ( $< 25\text{nm}$ ) at increased levels over background concentrations up to 18 km downwind. Riley et al. (2016) measured a three- to five-fold increase over background particle emissions (defined as the measured concentrations 5<sup>th</sup> percentile) at 5 and 10 km under the aircraft landing path at both LAX and Hartsfield-Jackson International (Atlanta). Landing operations happen over a longer period of time than takeoffs as aircraft arrive at the airport after a slow descent covering a wide area.

Engine type can affect the quantity and type of emissions. During a study at Oakland Airport, Lobo et al. (2012) found that older technology engines had as much as 3 times higher mass-based emission indices at takeoff compared with newer technology engines. However, the study does not compare older vs. newer engines of the same make and model. Additionally, UFP emissions differ between engine type for exhaust measurements in near field plumes (Kinsey et al., 2010; Timko et al., 2010b; Lobo et al., 2012). For gas turbine engines, the power setting and ambient conditions at the engine inlet influence emissions (Lobo et al., 2007).

### **UFP Measurements Downwind of Airport**

Wind speed and direction affect how far downwind measurements can be attributed to aircraft operations. Hu et al. (2009) determined UFP concentrations from aircraft at Santa Monica Airport (SMO) to be 10 and 2.5 times over the background levels at 100m and 660m, respectively. Additionally, UFP concentrations from SMO were measured in residential neighborhoods 80 to 400 m downwind (Choi et al., 2013). Elevated UFP counts were measured at a site 250 m downwind of LAX 1 minute after aircraft takeoff with baseline levels reached again 5 minutes after takeoff (Hsu et al. 2013). Zhu et al. (2011) were able to assign UFP peak concentrations to specific takeoffs 600 m downwind of the runway at LAX. These elevated particle counts, as well as increased BC concentrations, were higher than those measured at a background site (Zhu et al., 2011). At T.F. Green airport in Warwick, Rhode Island, aviation activities contributed 15 to 30 percent of UFP measured at two sites near the airport (between 0.16 km west of the main taxiway for the main runway and 0.3 km from the main runway) (Hsu et al., 2012).

### **Aircraft Mode Contributions**

The majority of emissions from idle and takeoff are higher than landing emissions. Multiple studies reported aircraft idle mode to be the highest source of emissions but to be dependent upon

the pollutant (Agrawal et al., 2008; Herndon et al., 2008). Incomplete combustion of aviation fuel happens during idle when thrust setting is lower and engine operations are at a lower temperature. Idle emission indices for HC and CO from aircraft engine emissions are an order of magnitude larger than takeoff settings for an engine (Agrawal et al., 2008; Herndon et al., 2008). PM emissions comprised a larger portion of takeoff and landing emissions than HC and CO (Agrawal et al., 2008). Thrust's effect on emission levels depends on aircraft settings (e.g., idle, takeoff, taxi, and landing). Mazaheri et al. (2011) observed PM<sub>2.5</sub> numbers and NO<sub>x</sub> concentrations to be highly dependent upon engine thrust level.

Emissions indices measurements are reported as mass of pollutant emitted per mass of fuel burned (g kg<sup>-1</sup>) and provide information on the pollutants in the fuel and the quantity in which they are emitted by setting, such as increase or decrease of thrust. Ultimately, the emission index can be used to calculate the total emissions of pollutant produced by a specific aircraft for one LTO cycle (ICAO, 2012)

The configuration of an airport's runways can affect time spent in each operational mode. A longer taxiing distance can lead to increased incomplete combustion and an increase of CO or unburned HC emissions. If the airport is prone to long delays for takeoff, aircraft can operate in idle mode longer, leading to increased emissions. Runway configuration also influences emissions as aircraft primarily take off into the wind. As an example, LAX aircraft operations primarily occur to the west with higher emissions measured east of the airport. With a predominant onshore breeze measured at LAX for most of the day, communities downwind of the airport are affected by emissions from both aircraft departures and arrivals.

## **International Civil Aviation Organization Measurements and Requirements**

Engine manufacturers are required to submit aircraft engine emissions to the International Civil Aviation Organization (ICAO) databank with annual updates, as necessary. Information on engine identification, rated thrust, reference pressure ratio, fuel specification reference, fuel hydrogen/carbon ratio, methods of data acquisition, method of making corrections for ambient conditions, and method of data analysis are provided (ICAO, 2008). The following test information must be submitted: fuel flow ( $\text{kg s}^{-1}$ ); emission index ( $\text{g kg}^{-1}$ ) for each gaseous pollutant; and measured Smoke Number (SN), which is an indicator of plume opacity (ICAO, 2008). From the test information, the emission rate (emission index  $\times$  fuel flow), total gross emission of each gaseous pollutant measured over LTO cycle, values of  $D_p/\text{Foo}$  for each gaseous pollutant, and maximum SN (ICAO, 2008) must be determined.  $D_p/\text{Foo}$  is the mass in grams of any pollutant emitted during the reference LTO cycle divided by the rated output of the engine. HC emissions measurements are done using a heated flame ionization detector (FID) and are expressed as a combined estimate of HC compounds in the exhaust gas. CO and CO<sub>2</sub> are measured using a non-dispersive infrared analyzer. NO<sub>x</sub> components are measured by a chemiluminescent method that measures radiation intensity emitted from the reaction of NO with added ozone to provide NO<sub>x</sub> concentration (ICAO, 2008). Calibration must occur prior to any testing.

Emissions measured for the ICAO database include unburnt HCs, CO, and NO<sub>x</sub> from turbojet and turbofan engines. Standards for gaseous emissions apply to engines with a rated output greater than 26.7 kilonewtons (kN). Manufacturers of aircraft engines complete their emissions testing by running the engine on a test bed at each thrust setting. The ICAO measurements require thrust setting for the LTO cycle to be: take-off (100 percent thrust); climb out (85 percent thrust); approach (30 percent thrust); and taxi/ground idle (7 percent thrust). For gaseous emissions

calculations, time in each LTO operating mode is required to be 7.7 minutes for takeoff, 2.2 minutes for climb out, 4 minutes for approach, and 26 minutes for taxi/ground idle.

Default assumptions for the LTO cycle include emissions assessed below 915 meters and the Dp/Foo values to be based on idealized cycles in International Standard Atmosphere (ISA) conditions. Rated output is the maximum thrust available for takeoff under normal operating conditions. Once the data are compiled from the engine testing, they are submitted to the primary certifying authority where, upon approval, the emissions data are submitted to ICAO for addition or revision in the databank. For NO<sub>x</sub>, CO, and HC, an average of four tests are conducted for the engine tests and two engines tested for each engine type.

The ICAO database includes emissions indices for NO<sub>x</sub>, CO, HC, and SN for idle, climb out, takeoff, and approach. The overall rated output of the engine in the database is also included as thrust in kN. In addition to the emissions index, the database includes the fuel flow (kg s<sup>-1</sup>) for each operation setting as well as fuel used per LTO cycle (in kg).

There are many drawbacks of the engine emissions measurements as required by ICAO. Engine emissions measurements tests are conducted on a test bed. Additionally, measurements do not account for how pollutants are dispersed in the atmosphere. The values for HC are only from those unburnt HCs, which could potentially lead to underestimation in the databank values. Also, the emission index is calculated for HCs but not HCHO (formaldehyde). Measurements for CO and NO<sub>x</sub> are subject to interference effects to a significant degree with a need to correct for sample drying. These effects are mainly caused by CO<sub>2</sub> and H<sub>2</sub>O in the sample, which cause the CO analyzer to be prone to zero shifting and the NO<sub>x</sub> analyzer to a sensitivity change (ICAO, 2008). Although these are corrected for during the measurement process, they can affect values submitted to the ICAO database.

## **Comparison of ICAO Emissions and Field Measured Values**

There are multiple studies where EI's are calculated from field measurements and compared with those in the ICAO database. Values in the ICAO database are assumed to be under ISA conditions, which can lead to over- and underestimates when compared with field measurements. NO<sub>x</sub> EI measurements were found to be between 10 and 15 percent lower than those values in the ICAO database, which leads to an overestimation in the ICAO database (Herndon et al., 2005; 2008; Timko et al., 2010a). Herndon et al. (2009) reported a calculated EI value for CO was underestimated in the ICAO database. Additional studies reported that calculated BC and particle number EIs were lower than those values found in the ICAO database, which leads to an overestimation of emissions (Klapmeyer and Marr, 2012). HC emissions can be underestimated in idle mode by 16-45 percent (Herndon et al., 2009).

The ICAO testing requirements assign 7 percent thrust rating for both idle and taxiing. However, Mazaheri et al. (2009) found thrust levels to be higher during taxiing than idling mode. This can affect ICAO database values, with higher thrust during field measurements leading to higher emission levels or different types of emissions, such as composition of unburnt HC, which depend on heat and thrust. Additionally, ICAO idle emissions are an average for aircraft at the entire airport and include a mixture of both true idling as well as taxiing (Schurmann et al., 2007). This can also lead to an underestimate of CO and an overestimate of NO<sub>x</sub> due to lower thrust during true idling (Schurmann et al., 2007). For takeoff mode in ICAO engine testing, engines operate at 100 percent thrust. However, engines often do not operate at full thrust to conserve fuel during takeoff.

When real time measurements are compared to those in the ICAO database, they tend to be over- or underestimated. However, ICAO parameters can provide emission values when field tests

are unavailable. These values can potentially be used to help determine other pollutant values, such as using ICAO parameters to correlate and predict a pollutant not included in the database. Multiple studies have reported particle and NO<sub>x</sub> emissions exhibit an almost linear relationship with the level of thrust from an engine (Mazaheri et al., 2009; Rice, 2001; Petzold et al., 1999; Petzhold and Schroder, 1998).

### **UFP, Health, and ICAO Database Parameters**

The ICAO database contains measurements for NO<sub>x</sub>, unburned HC, and CO, but no emission index or fuel flow metric for ultrafine particles (UFP). UFPs have the numbers and surface area to carry adsorbed or condensed toxic air pollutants (Delfino et al., 2005). Studies have reported UFP can reach cardiovascular target sites and cause systemic inflammation (Delfino et al., 2005), which can lead to increased blood pressure or myocardial infarction. Additionally, exacerbation of asthma in asthmatics can be triggered due to oxidative stress and inflammation caused by UFP (Weichenthal et al., 2007; Knibbs et al., 2011). Increased UFP concentrations can cause a reduction in lung function and increase daily symptoms in asthmatics and chronic obstructive pulmonary diseased (COPD) patients (Wichmann et al., 2000; Ibald-Mulli et al., 2002; Knibbs et al., 2011). UFP respiratory affects include a decrease in forced expiratory volume in asthmatic children (Pekkanen et al., 1997).

Particulate emissions from aircraft have been attributed to both takeoff and landing operations at multiple airports (Unal et al., 2005; Westerdahl et al., 2008; Hu et al., 2009; Zhu et al., 2011; Hsu et al., 2012; 2013; 2014; Choi et al., 2013; Hudda et al., 2014; Keuken et al., 2015; Hudda and Fruin, 2016; Moore et al., 2017) with a smaller number of studies being able to assign specific peak UFP concentrations to specific aircraft takeoffs (Westerdahl et al., 2008; Zhu et al., 2011). UFP concentrations have also been measured in communities adjacent to and far downwind of



airports (Westerdahl et al., 2008; Hsu et al., 2014; Keuken et al., 2015; Hudda et al., 2014; Hudda and Fruin, 2016; Riley et al., 2016). While the health impacts resulting from UFP from aircraft are not fully understood, other studies suggest UFP are responsible for adverse health effects (Peters et al., 1997; Oberdorster, 2000; Penttinen et al., 2001; Delfino et al., 2005; Hoek et al., 2010). Further study into the impact of UFP from aircraft operations can help to elucidate the health impacts from these smallest particles.

## References

- Agrawal H, Sawant AA, Jansen K, Miller JW, and DR Cocker III. 2008. Characterization of chemical and particulate emissions from aircraft engines. *Atmospheric Environment*. 42(18): 4380-4392.
- Brock CA, Schroder F, Karcher B, Petzold A, Busen R, and Fiebig M. 2000. Ultrafine particle size distributions measured in aircraft exhaust plumes. *Journal of Geophysical Research: Atmospheres*. 105:D21 p. 26555-26567.
- Carslaw DC, Beevers SD, Ropkins K, and MC Bell. 2006. Detecting and quantifying aircraft and other on-airport contributions to ambient nitrogen oxides in the vicinity of a large international airport. *Atmospheric Environment* 46: 5424-5434.
- Choi W, Hu S, He M, Kozawa K, Mara S, Winer AM, and SE Paulson. 2013. Neighborhood-scale air quality impacts of emissions from motor vehicles and aircraft. *Atmospheric Environment*. 80: 310-321.
- Dodson RE, Houseman EA, Morin B, and JI Levy. 2009. An Analysis of Continuous Black Carbon Concentrations in Proximity to an Airport and Major Roadways. *Atmospheric Environment*.
- Delfino RJ, Sioutas C, and S Malik. 2005. Potential Role of Ultrafine Particles in Associations between Airborne Particle Mass and Cardiovascular Health. *Environ. Health Perspect.* 113(8): 934-946.
- Federal Aviation Administration. *Aviation Emissions, Impacts & Mitigation: A Primer*. FAA Office of Environment and Energy. January 2015.
- Federal Aviation Administration. *Aviation Maintenance Technician Handbook – Airframe*. Volume II. Chapter 14: Aircraft Fuel Systems. 2012.

- Herndon SC, Wood EC, Northway MJ, Miake-Lye R, Thornhill L, Beyersdorf A, Anderson BE, Dowlin R, Dodds W, and WB Knighton. 2009. Aircraft Hydrocarbon Emissions at Oakland International Airport. *Environ. Sci. Technol.* 43: 1730-1736.
- Herndon SC, Jayne JT, Lobo P, Onasch TB, Fleming G, Hagen DE, Whitefield PD, and RC Miake-Lye. 2008. Commercial Aircraft Engine Emissions Characterization of in-Use Aircraft at Hartsfield-Jackson Atlanta International Airport. *Environ. Sci. Technol.* 42(6): 1877-1883.
- Herndon SC, Onasch TB, Frank BP, Marr LC, Jayne JT, Canagaratna MR, Grygas J, Lanni T, Anderson BE, Worsnop D, and RC Miake-Lye. 2005. Particulate Emissions from in-use Commercial Aircraft. *Aerosol Science and Technology.* 39(8): 799-809.
- Hoek G, Boogaard H, Knol A, De Hartog J, Slottje P, Ayres JG, Borm P, Brunekreef B, Donaldson K, Forastiere F, Holgate S, Kreyling WG, Nemery B, Pekkanen J, Stone V, Wichmann HE, and J Van Der Sliujs. 2010. Concentration response functions for ultrafine particles and all-cause mortality and hospital admissions: Results of a European expert panel elicitation. *Environ. Sci and Technol.* 44(1): 476-482.
- Hsu HH, Adamkiewicz G, Houseman EA, Spengler JD, and JI Levy. 2014. Using mobile monitoring to characterize roadway and aircraft contributions to ultrafine particle concentrations near a mid-sized airport. *Atmospheric Environment.* 89: 688-695.
- Hsu HH, Adamkiewicz G, Houseman EA, Zarubiak D, Spengler JD, and JI Levy. 2013. Contributions of aircraft arrivals and departures to ultrafine particle counts near Los Angeles International Airport. *Science of the Total Environment.* 444. 347-355.
- Hsu HH, Adamkiewicz G, Houseman EA, Vallarino J, Melly SJ, Wayson RL, Spengler JD, and JI Levy. 2012. The relationship between aviation activities and ultrafine particulate matter concentrations near a mid-sized airport. *Atmospheric Environment.* 50: 328-337.

- Hu S, Fruin S, Kozawa K, Mara S, Winer AM, and SE Paulson. 2009. Aircraft Emission Impacts in a Neighborhood Adjacent to a General Aviation Airport in Southern California. *Environ. Sci. Technol.* 43. 8039-8045.
- Hudda H and SA Fruin. 2016. International Airport Impacts to Air Quality: Size and Related Properties of Large Increases in Ultrafine Particle Number. *Environ. Sci. Technol.* 50. 3362-3370.
- Hudda N, Gould T, Hartin K, Larson TV, and S Fruin. 2014. Emissions from an International Airport Increase Particle Number Concentrations 4-fold at 10 km downwind. *Environ. Sci. Technol.* 48. 6628-6635.
- Ibald-Mulli, A., Wichmann, H.E., Kreyling, W., Peters, A., 2002. Epidemiological Evidence on Health Effects of Ultrafine Particles. *Journal of Aerosol Medicine* 15, 189-201.
- International Civil Aviation Organization. 2012. Airport Air Quality Manual. Doc 9889 First Edition Corrigendum No. 1.
- International Civil Aviation Organization. 2008. ICAO Annex 16: Environmental Protection, Volume II – Aircraft Engine Emissions. International Standards and Recommended Practices.
- IPCC. 1999. Aviation and the Global Atmosphere. Chapter 3. Section 3.2. Aerosol Emission and Formation in Aircraft Plumes (<http://www.ipcc.ch/ipccreports/sres/aviation/index.php?idp=31>)
- Kapadia ZZ, Spracklen DV, Arnold, SR, Borman DJ, Mann GW, Pringle KJ, Monks SA, Reddington CL, Benduhn R, Rap A, Scott CE, Butt EW, and M Yoshioka. 2015. Impacts of aviation fuel sulfur content on climate and human health. *Atmos. Chem. Phys. Discuss.* 15: 18921-18961.

- Keuken MP, Moerman M, Zandveld P, Henzing JS, and G Hoek. 2015. Total and size-resolved particle number and black carbon concentrations in urban areas near Schiphol airport (the Netherlands). *Atmospheric Environment*. 104: 132-142.
- Kinsey JS, Hays MD, Dong Y, Williams DC, and R Logan. 2011. Chemical Characterization of the Fine Particle Emissions from Commercial Aircraft Engines during the Aircraft Particle Emissions eXperiment (APEX) 1 to 3. *Environ. Sci. Technol.* 45(8): 3415-3421.
- Kinsey JS, Dong Y, Williams DC, and R Logan. 2010. Physical characterization of the fine particle emissions from commercial aircraft engines during the Aircraft Particle Emissions eXperiment (APEX) 1-3. *Atmospheric Environment*. 44(17): 2147-2156.
- Klapmeyer ME and LC Marr. 2012. CO<sub>2</sub>, NO<sub>x</sub>, and Particle Emissions from Aircraft and Support Activities at a Regional Airport. *Environ. Sci. Technol.* 46(20): 10974-10981.
- Knibbs LD, Cole0Hunter T, and L Morawska. 2011. A review of commuter exposures to ultrafine particles and its health effects. *Atmospheric Environment*. 45(16) 2611-2622.
- Lobo P, Hagen DE, and PD Whitefield. 2012. Measurements and analysis of aircraft engine PM emissions downwind of an active runway at the Oakland International Airport. *Atmospheric Environment*. 61: 114-123.
- Lobo P, Hagen DE, Whitefield PD, and DJ Alofs. 2007. Physical Characterization of Aerosol Emissions from a Commercial Gas Turbine Engine. *Journal of Propulsion and Power*. 23(5): 919-929.
- Mazaheri M, Johnson GR, and L Morawska. 2011. An inventory of particle and gaseous emissions from large aircraft thrust engine operations at an airport. *Atmospheric Environment*. 45(20): 3500-3507.

- Mazaheri M, Johnson GR, and L Morakawa. 2009. Particle and Gaseous Emissions from Commercial Aircraft at Each Stage of the Landing and Takeoff Cycle. *Environ. Sci. Technol.* 43. 441-446.
- Moore RH, Shook MA, Ziemba LD, DiGangi JP, Winstead EL, Rauch B, Jurkat T, Thornhill KL, Crosbie EC, Robinson C, Shingler TJ, and BE Anderson. 2017. Take-off engine particle emission indices for in-service aircraft at Los Angeles International Airport. *Scientific Data.* 4: 170198 doi: 10.1038/sdata.2017.198 (198)
- Oberdorster G. 2000. Pulmonary effects of inhaled ultrafine particles. *International Archives of Occupational and Environmental Health.* 74(1): 1-8.
- Onasch TB, Jayne JT, Herndon S, Worsnop DR, and RC Miake-Lye. 2009. Chemical Properties of Aircraft Engine Particulate Exhaust Emissions. *Journal of Propulsion and Power.* 25(5): 1121-1137.
- Peters A, Wichmann HE, Tuch T, Heinrich H, and J Heyder. 1997. Respiratory Effects Are Associated with the Number of Ultrafine Particles. *Am J Respir Crit Care Med.* 155: 1376-1383.
- Pekkanen J, Timonen KL, Ruuskanen J, Reponen A, and A Mirme. 1997. Effects of ultrafine and fine particles in urban air on peak flow expiratory flow among children with asthmatic symptoms. *Environ Res.* 74:24–33.
- Penttinen P, Timonen KL, Tittanen P, Mirme A, Ruuskanen J, and J Pekkanen. 2001. Ultrafine particles in urban air and respiratory health among adult asthmatics. *European Respiratory Journal.* 17: 428-435.

- Petzold, A.; Strom, J.; Schroder, F. P.; Karcher, B. Carbonaceous aerosol in jet engine exhaust: emission characteristics and implications for heterogeneous chemical reactions. *Atmos. Environ.* 1999, 33 (17), 2689–2698.
- Petzold, A.; Schroder, F. P. Jet engine exhaust aerosol characterization. *Aerosol Sci. Technol.* 1998, 28 (1), 62–76.
- Ratliff G, Sequeira C, Waitz I, Ohsfeldt M, Thrasher T, Graham M, and T Thompson. 2009. Aircraft Impacts on Local and Regional Air Quality in the United State. PARTNER Project 15 final report.
- Rice, CC. Restricting the Use of Reverse Thrust as an Emissions Reduction Strategy. The University of Texas at Austin: Austin, 2001.
- Riley EA, Gould T, Hartin K, Fruin SA, Simpson CD, Yost MG, and T Larson. 2016. Ultrafine particle size as a tracer for aircraft turbine emissions. *Atmospheric Environment*. 139. 20-29.
- Schurmann G, Schafer K, Jahn C, Hoffman H, Bauerfeind M, Fleuti E, and B Rappengluck. 2007. The impact of NO<sub>x</sub>, CO, and VOC emissions on the air quality of Zurich airport. *Atmospheric Environment*. 41: 103-118.
- Timko MT, Herndon SC, Wood EC, Onasch TB, Northway MJ, Jayne JT, Canagaratna MR, Miake-Lye RC, and WB Knighton. 2010a. Gas Turbine Engine Emissions – Part 1: Volatile Organic Compounds and Nitrogen Oxides. *J. Eng. Gas Turbines Power*. 132(6): 061504-1 – 14.
- Timko MT, Onasch TB, Northway MJ, Jayne JT, Canagaratna MR, Herndon SC, Wood EC, Miake-Lye RC, and WB Knighton. 2010b. Gas Turbine Engine Emissions – Part II:

Chemical Properties of Particulate Matter. *J. Eng. Gas Turbines Power* 132(6): 061505-1  
– 15.

Unal A, Hu Y, Change ME, Odman MT, and AG Russell. 2005. Airport related emissions and impacts on air quality: Application to the Atlanta International Airport. *Atmospheric Environment*. 39: 5787-5798.

Weichenthal, S., Dufresne, A., Infante-Rivard, C., 2007. Indoor ultrafine particles and childhood asthma: exploring a potential public health concern. *Indoor Air* 17, 81-91.

Westerdahl D, Fruin SA, Fine PL, and Sioutas C. 2008. The Los Angeles International Airport as a source of ultrafine particles and other pollutants to nearby communities. *Atmospheric Environment*. 42: 3143-3155

Wichmann, H.E., Peters, A., 2000. Epidemiological evidence of the effects of ultrafine particle exposure. *Philosophical Transactions of the Royal Society of London. Series A: Mathematical, Physical and Engineering Sciences* 358, 2751-2769.

Yu KN, Cheung YP, Cheung T, and RC Henry. 2004. Identifying the impact of large urban airports on local air quality by nonparametric regression. *Atmospheric Environment*. 38: 4501-4507.

Zhu Y, Fanning E, Yu RC, Zhang Q, and JR Froines. 2011. Aircraft emissions and local air quality impacts from takeoff activities at a large International Airport. *Atmospheric Environment*. 45: 6526-6533.



# Use of International Civil Aviation Organization Database Parameters to Determine UFP Concentrations at Santa Monica Airport

Erica Alvarado<sup>1</sup> and Suzanne E. Paulson<sup>2</sup>

1. Air Quality Group. Tetra Tech, Inc. 3475 East Foothill Blvd., Pasadena, CA 91107
2. Department of Atmospheric and Oceanic Sciences, University of California Los Angeles, Los Angeles, CA 90095-1772, USA

## Abstract

Emissions from aircraft operations can substantially increase concentrations of several pollutants in communities near airports. Aircraft produce a range of pollutants, including oxides of nitrogen, carbon monoxide, black carbon, volatile organic compounds, and ultrafine particles (UFP). Several of these, especially UFP and black carbon, can result in concentrations that are several times higher than typical urban backgrounds for extended areas around airports. Aircraft engines are tested for emissions of several pollutants, but none of the tests are specifically aimed at UFP. A data set collected by the South Coast Air Quality Management District (SCAQMD) from September 12 through October 3, 2010 was analyzed to determine peak UFP concentrations associated with individual takeoff and landing operations. We then associated each operation with specific aircraft, including engine characteristics, engine age, and engine emission rates published in the International Civil Aviation Organization (ICAO) database parameters (nitrogen oxides [NO<sub>x</sub>], carbon monoxide [CO], hydrocarbons [HC], smoke number [SN], and engine thrust). ICAO emissions data were compared with measured UFP concentrations to determine which, if any, parameters are predictive for UFP concentrations from specific aircraft. UFP peak concentrations associated with both takeoff and landing operations at the airport were identified, with peaks more clearly defined for takeoff operations. A single variable linear regression run for each ICAO parameter separately for takeoff and landing UFP peak concentrations found NO<sub>x</sub> and thrust to be

strongly correlated with all emission rates for takeoff operations. CO was significant for takeoff and climbout, SN was significant for takeoff, approach, and idle, and HC was significant for climbout only. At the sampling location (100 m from the end of the runway) takeoff operations result in 60 percent higher pollutant concentrations than landings. Finally, no evidence was observed for significant changes in aircraft emissions and fleet ages.

## 1. Introduction

While the full range of health impacts of ultrafine particles (UFPs) are not well understood, many studies reported an increased risk in cardiovascular disease as well as pulmonary functioning when exposed to higher levels of UFP (Peters et al., 1997; Oberdorster, 2000; Chalupa et al., 2004; Delfino et al., 2005; Gong et al., 2008). Increases in UFP pollution have been linked to increases in respiratory and cardiovascular morbidity, such as increased hospitalization, and mortality (Peters et al., 1997; Delfino et al., 2005; Hoek et al., 2010). Respiratory problems, specifically asthma and its symptoms, are worsened by an increase in UFP concentrations (Chalupa et al., 2004; Pietropaoli et al., 2004; Gong et al., 2008).

Aircraft have been shown to be efficient emitters of UFP, with much higher UFP/kilogram (kg) than motor vehicles. Hu et al. (2009) measured UFP emissions from aircraft at a small general aviation airport (Santa Monica Airport [SMO]), and estimated aircraft emissions contained approximately  $5 \times 10^{16}$  particles/kg fuel consumed. Other studies reported large aircraft emissions to emit between  $0.3\text{-}5 \times 10^{16}$  particles/kg fuel consumed (Herndon et al., 2005; Lobo et al., 2007). While the estimate by Hu et al. (2009) is on the higher end of aircraft emissions per particles/kg of fuel consumed, it was 16-100 and 5-8 times higher than UFP emitted per kg fuel consumed by light and heavy duty diesel trucks, respectively (Kirschstetter et al., 1999; Hu et al., 2009; Westerdahl et al., 2009).

Spikes in UFP number concentrations have been found by several studies to correlate to takeoff operations and often, specific takeoff events (Westerdahl et al., 2008; Hu et al., 2009; Zhu et al., 2011; Choi et al., 2013; Keuken et al., 2015; Moore et al., 2017). A smaller number of studies have examined landing operations, and have found that landings can also contribute to elevated UFP concentrations downwind of an airport (Westerdahl et al., 2008; Hsu et al., 2014; Keuken et al.,

2015; Hudda and Fruin, 2016; Riley et al., 2016). Westerdahl et al. (2008) observed UFP particle count peaks corresponding to individual aircraft landing operations 500 m downwind of LAX. Aircraft preferentially takeoff and land into the prevailing wind, thus the downwind area is commonly below the arrival path, more so near airports.

A small number of studies have looked at UFP impacts from small general aviation airports, particularly Santa Monica Airport (SMO) (Hu et al., 2009; SCAQMD, 2011; Choi et al., 2013). SMO is a municipal airport located in the City of Santa Monica, California and is surrounded on all sides by dense residential neighborhoods. Approximately 300 aircraft are based at the airport with an average of 230 daily operations (SMO, 2017a). Measurements have repeatedly shown large increases in UFP in the community downwind of the airport (Hu et al., 2009; Choi et al., 2013). While jet traffic had been increasing since 2012, with jets contributing 22 percent of total operations at the airport in 2016 (SMO 2017a); a recent project in December 2017 shortened the runway from 4,973 to 3,500 feet, thereby reducing jet traffic by over 80 percent (SMO, 2017b).

The Council of International Civil Aviation Organization (ICAO) has adopted engine certifications standards that aircraft are required to meet. The requirement exists for regulated engines which are turbojet and turbofan engines newer than engine model year 1986 with a static thrust rating greater than 26.7 kilonewtons (kN) for gaseous emissions and engine model year newer than 1983 for smoke (ICAO, 2018). Standards include limits on emissions of oxides of nitrogen ( $\text{NO}_x$ ), carbon monoxide (CO), hydrocarbons (HCs), and smoke number (SN) (a measure of the emission cloud opacity) for a reference landing and take-off (LTO) cycle below 3000 feet (ft). The emissions data are maintained in the ICAO database (ICAO, 2012). Data in the database are provided by manufacturers and specific measurement techniques are specified by ICAO. Smaller aircraft engines are not required to submit to the ICAO database. ICAO measurements are

required for LTO operating modes including take-off (100 percent thrust); climb out (85 percent thrust); approach (30 percent thrust); and taxi/ground idle (7 percent thrust).

Here, UFP data collected by the South Coast Air Quality Management District (SCAQMD) and aircraft operations data from the City of Santa Monica are probed to explore the relationships between observed UFP concentrations and published emissions and engine characteristics. The SMO data are at a high enough time resolution to resolve UFP peaks associated with individual takeoff and landing operations. Provided aircraft tail numbers were used to retrieve specific emissions and thrust data for individual engines. Correlations between the ICAO parameters as well as engine age and thrust and peak UFP concentrations for both takeoff and landing were investigated. Additionally, the characteristics of UFP from takeoff versus landing are explored.

## **2. Methods**

### **2.1 Sites**

SMO occupies 227 acres and is surrounded by dense residential neighborhoods on all sides. Two primary sites included the East Tarmac (or Runway or RW) site located 35 m north of the end of the runway and a Residential Backyard Site (the Ernst site) located approximately 100 m northeast of the end of the runway (SCAQMD, 2011). Continuous UFP and black carbon (BC) measurements were collected at these two sites at 1- and 5-minute intervals, respectively. UFP and BC measurements were also collected indoors at the Residential site. Additionally, continuous 1-minute non-methane hydrocarbons (NMHCs) and 5-minute canister samples for volatile organic compound (VOC) analysis were collected at two mobile monitoring stations located at the East Tarmac and Ernst Residential sites (Fig. 1).

The runways are oriented at 220° (Fig. 1) with aircraft taking off and landing to the west over 95% of the time. This places the Runway and Ernst sites slightly to the north of the end of the runways and directly downwind of the end of the runways, respectively.

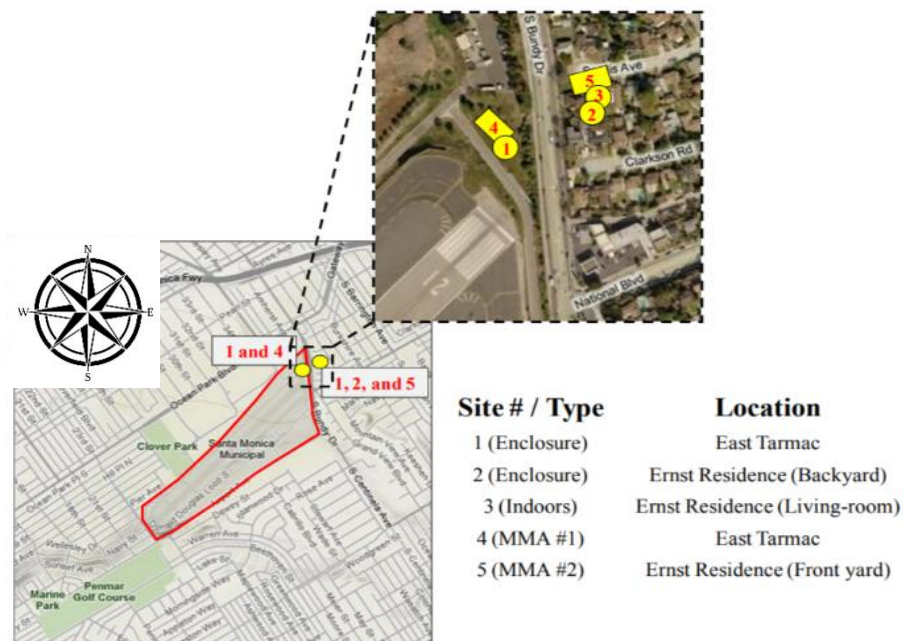


Figure 1. Study area for SCAQMD Supplemental Study (2011). Sites 1 and 2 were used for this analysis. Site 1 is the East Tarmac (RW site) and Site 2 is the Ernst site. Site 3 was the Indoor Site located at the Ernst residence. Sites 4 and 5 were two mobile monitoring stations deployed at the RW site (Site 4) and the Ernst site (Site 5).

#### *UFP Measurements*

One-minute UFP data were collected from September 12 – 24, 2010 and September 27 – October 3, 2010. UFP data were unavailable from September 24 – 27, 2010 due to instrument problems. The main objective of the SCAQMD study was to further understand short-term impacts of aircraft emissions on neighboring communities and to take advantage of a “natural experiment” during which the airport was closed from September 19 – 24, 2010. UFP measurements were collected with a Water-based Condensation Particle Counter (CPC; TSI Model 3785), which has

a single-particle-counting mode with a temperature-stabilized photometric mode (TSI, 2018). The CPCs are able to measure UFP number concentrations up to 10,000,000 # cm<sup>-3</sup> (SCAQMD, 2011).

### *Wind Speed and Direction*

Hourly meteorological data, including wind speed and direction, were obtained from MesoWest (<http://mesowest.utah.edu/>) for the KSMO site located at SMO. Data falling outside the 180 - 260° wind direction range (roughly downwind of the airport) were removed from the dataset. Eighty-nine percent of all takeoff and 86 percent of all landing data fell in the 180-260° range. The average wind speed was ± 3 m/s, thus the average transport time to the Ernst site was approximately 30 seconds.

## 2.2 SMO Operations

Data were collected from September 12, 2010 to October 3, 2010. Flight activity and aircraft tail number data were obtained from the City of Santa Monica. SCAQMD collected takeoff, idle, and hold times, aircraft type and registration, and engine type (turbo or jet; piston aircraft were not tracked) for each takeoff operation. The aircraft landing operations data for the period of the study were obtained from the airport via the City of Santa Monica, and included landing times and aircraft information (registration [N-Number], aircraft and engine type, and runway used).

The aircraft information was queried in the FAA N-Number Inquiry database to identify engine manufacturer, model, and manufacture year (FAA, 2017), and matched to aircraft operations. Some engine model information was unavailable because aircraft had been deregistered by the time the database was queried or the engine model information in the database was not sufficiently specific. Table 1 shows the data availability by category. For aircraft not in the ICAO database, we contacted engine manufacturers directly or obtained engine thrust data from company websites.

**Table 1. Data Set Utilized for Study**

<b>Data Set</b>	<b>Aircraft Operations</b>
Total Operations Observed	370 Takeoff 374 Landing
Operations with UFP and Thrust Available	104 Takeoff 65 Landing
Operations with UFP and ICAO Parameters Available	51 Takeoff 31 Landing

### *ICAO Emissions Database*

Aircraft engine types were linked with the ICAO database. The database is limited to engine types with thrust ratings above 26.7 kN and included specific engine models from Pratt & Whitney, Rolls Royce, Honeywell, GE, CFM International, and Allied Design.

Data in the ICAO records include engine thrust (kN), emission indices ( $\text{g kg}^{-1}$ ), and fuel flow rates ( $\text{kg s}^{-1}$ ) for landing/takeoff (LTO) cycle for hydrocarbons (HC), nitrogen oxides ( $\text{NO}_x$ ), carbon monoxide (CO), and smoke number (SN).

The provided emission index (EI) and fuel flow rate for each LTO component (takeoff, climbout, approach, and idle) were used to determine the emission rates.

$$\text{EI (g kg}^{-1}\text{)} \times \text{Fuel Flow (kg s}^{-1}\text{)} = \text{Emission Rate (g s}^{-1}\text{)}$$

## **3. Results and Discussion**

### *3.1 Takeoff versus Landing*

Spikes in UFP concentrations could generally be assigned to a specific takeoff or landing, and usually appeared within  $\pm 5$  minutes before and after a takeoff or landing operation. Figures 2 and 3 show plots of the UFP concentrations for  $\pm 5$  minutes for takeoff and landing operations, respectively. Peaks associated with takeoffs were typically sharper than for landing; both types were usually symmetric.



Average takeoff peak width was 2.2 and 2.5 minutes for the RW and Ernst sites, respectively.

For arrivals, the average peak widths were 2.3 and 3.2 for the RW and Ernst Sites, respectively.

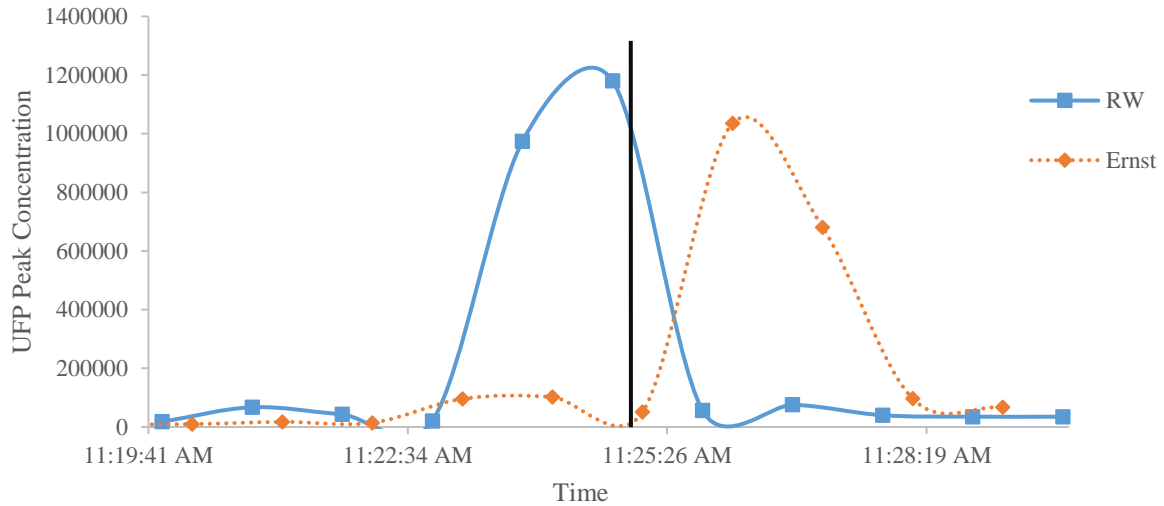


Figure 2. UFP concentrations  $\pm$  5 minutes from a sample takeoff. The black line indicates the recorded takeoff time of aircraft N256FX.

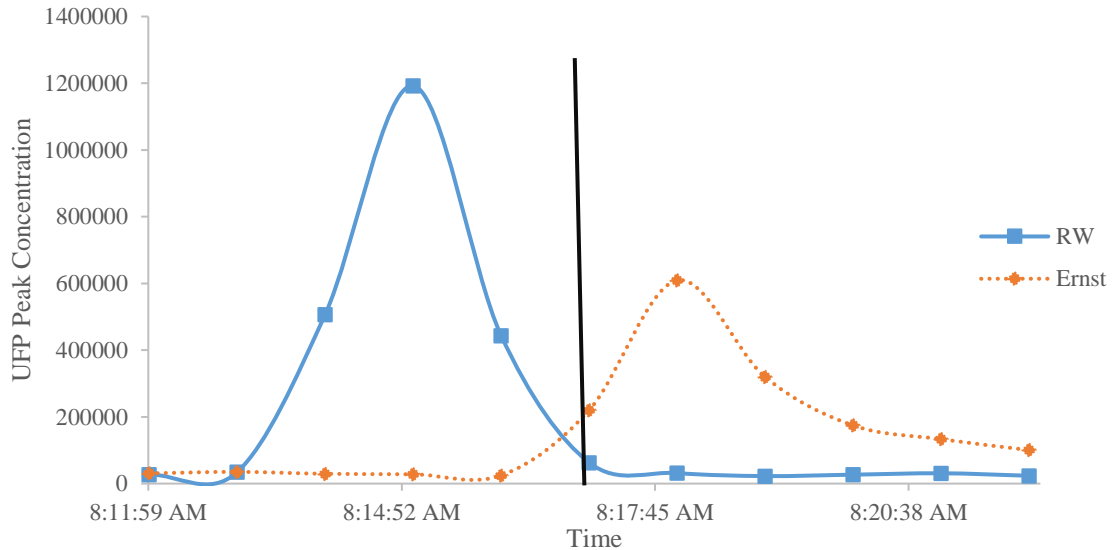


Figure 3. UFP concentrations  $\pm$  5 minutes from a sample arrival event. The black line indicates the recorded landing time of aircraft N204PT.

Table 2 shows the average UFP concentrations for takeoff and landing at the Ernst and RW sites. UFP peak concentrations were significantly higher for takeoff than landing operations at both

sites ( $p < 0.001$ ). At the Ernst Site, UFP concentrations from takeoff operations were 60% higher than landings (Table 2). Thrust at takeoff is close to 100% while thrust during landing is approximately 30%, which should lead to roughly 70% higher emissions for takeoff than landing, which is similar to what was observed here. This is in agreement with multiple studies that have reported higher emission rates for higher thrust and increased engine power (Agrawal et al., 2008; Wey et al., 2006; 2007; Mazaheri et al., 2009; Lobo et al., 2012). However, many of these studies were ground-based engine studies looking at direct emissions from an engine without much time for dilution of the plume. In contrast, Lobo et al. (2012) took measurements of idle/taxi and takeoff emissions between 100 - 300 m downwind of an active taxi area and runway at Oakland Airport. Idle/taxi emissions were measured much closer to the source to account for dispersion and found that number-based emission indices were similar between takeoff and taxi/idle ( $4 \times 10^{15} - 2 \times 10^{17}$  and  $7 \times 10^{15} - 3 \times 10^{17}$ , respectively) with taxi/idle slightly higher.

**Table 2. Average UFP Peak Concentrations by Site**

<b>SITE</b>	<b>Average UFP Peak Concentration – Takeoff</b>	<b>Average UFP Peak Concentration - Landing</b>
RW	379,000	119,000
ERNST	261,000	107,000

Comparison of UFP concentrations prior to, during, and after the airport closure from September 19 – 24, 2010 is included in the Appendix.

### 3.2 *Difference between Sites*

The RW site is located closer to the end of the runway than the Ernst sites and thus is expected to record takeoff concentrations before the Ernst site. As expected, UFP peak concentrations measured at the RW site were significantly higher than the Ernst site for takeoff operations, although they were also more variable as the sensor was not directly downwind, thus some peaks largely missed the RW sensor. There was no significant difference in UFP concentrations between

the two sites for landing operations. Studies that observed high UFP concentrations from landing emissions (Westerdahl et al., 2008; Hudda et al., 2014; Hudda and Fruin, 2016), have not directly compared UFP concentrations between two separate sites for the same airport.

UFP peak concentrations were on average  $1 \pm 1.2$  minutes prior to departure at the RW site and  $1.8 \pm 1.4$  minutes after departure at the Ernst site, a somewhat larger than expected separation considering the approximately 30 second average transport time to the site. For landing, UFP concentrations peaked at  $0 \pm 1.6$  at the RW site and  $1.1 \pm 2.0$  minutes after the recorded landing time at the Ernst site. This implies that the impact from landing is a combination of the Ernst site contributions from when the aircraft is overhead and from when the aircraft is close to landing or has already touched down. Hudda and Fruin (2016) measured landing emissions sooner than expected due to experiencing enhanced vertical mixing, thus allowing emissions to reach the ground sooner.

During the study season, some aircraft took off and landed repeatedly, and the assigned peaks varied widely, by factors of 3 – 12 for takeoff and 1 – 10 for landing. While some studies were able to assign peak UFP concentrations to specific aircraft operations (Westerdahl et al., 2008; Zhu et al., 2011), there is no evidence in the literature assigning UFP peak values to a specific aircraft for multiple takeoffs and landings. Further comparison of multiple operations for a single aircraft is included in the Appendix.

### 3.3 *ICAO Parameters and Operations*

Single variable linear regressions done for each emission rate of the LTO components were used to examine which variable best predicts UFP concentrations from takeoff and landing. Table 3 contains the resulting coefficients, significance,  $R^2$  values, and sample sizes for UFP peak concentrations from takeoff operations. Sample sizes differ between pollutants because some

emission rate values for specific engines are not included or are a 0 value in the ICAO database. Thrust is reported in the ICAO database as thrust rating; therefore, there was one overall value for thrust and no specific value for each of the LTO components. Correlation between ICAO parameters is further discussed in the Appendix.

**Table 3. Linear Regression Coefficients and p-values for ICAO Emission Rates and UFP Peak Concentrations**

		<b>Takeoff Emission Rate</b>	<b>Climbout Emission Rate</b>	<b>Approach Emission Rate</b>	<b>Idle Emission Rate</b>
<b>NO<sub>x</sub></b>	<b>coeff</b>	34,800**	53,500**	406,000**	1,950,000***
	<b>R<sup>2</sup> value</b>	(0.14)	(0.14)	(0.13)	(0.16)
<b>CO</b>		1,140,000***	1,200,000***	-40,200	105,000
		(0.23)	(0.29)	(-0.01)	(0.01)
<b>HC</b>		-517,000	-705,100	-161,000	-99,700
		(0.01)	(0.25)	(0.07)	(0.05)
<b>SN</b>		-26,000***	-27,300	-40,600*	-136,000*
		(0.17)	(0.15)	(0.14)	(0.17)
<b>Thrust</b>		11,000***			
		(0.22)			
<b>Sample Size</b>		NO <sub>x</sub> : 49	NO <sub>x</sub> : 49	NO <sub>x</sub> : 49	NO <sub>x</sub> : 49
		CO: 35	CO: 42	CO: 49	CO: 49
		HC: 37	HC: 45	HC: 39	HC: 49
		SN: 47	SN: 33	SN: 33	SN: 33

\*p<0.05, \*\*p<0.01, \*\*\*p<0.001

NO<sub>x</sub> and thrust are the best predictors for UFP peak concentrations from takeoff operations. NO<sub>x</sub> emission rates for all components of the LTO cycle are significant. A review by Masiol and Harrison (2014) reported findings that NO<sub>x</sub> emissions increase with an increase in engine thrust. Since engine thrust is highest for takeoff emissions, the finding that NO<sub>x</sub> and thrust are strong predictors for takeoff UFP concentrations agrees with other studies findings of higher thrust corresponding to higher NO<sub>x</sub> emissions.

Figures 4 and 5 show the variability in thrust and NO<sub>x</sub> ICAO values versus UFP peak concentrations assigned to aircraft takeoff operations. While the regression results in Table 3 show

that thrust is a significant predictor of UFP peak concentrations for takeoff emissions, it does not explain all variability in the peak concentrations. Wind direction influences peak concentrations with peak concentrations measured directly downwind of the airport runway and little to no influence when the site is upwind. Hudda et al. (2014) measured UFP concentrations upwind of LAX and found the concentrations to be typical of a coastal baseline concentration. Other influences include aircraft make, model, and operational mode.

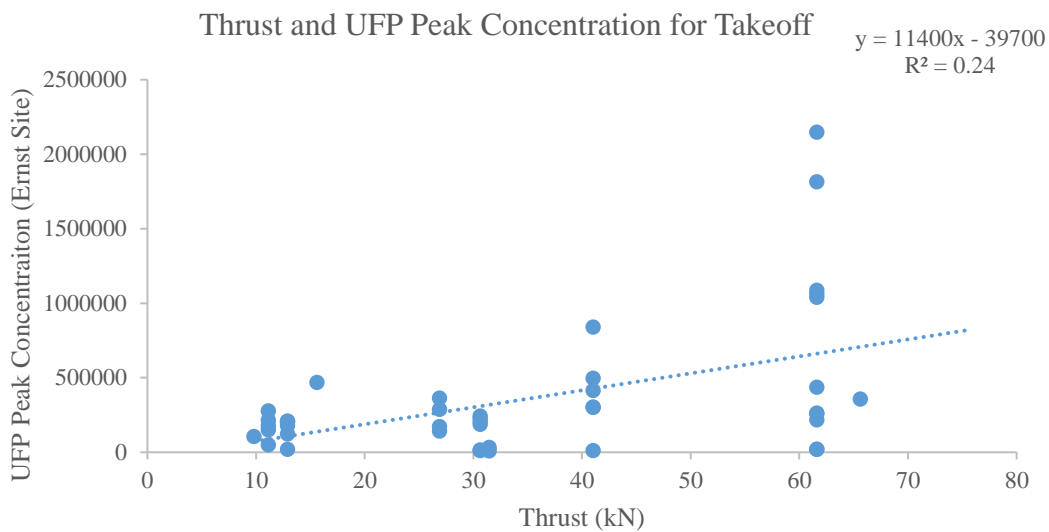


Figure 3. Thrust (kN) and UFP peak concentrations at the Ernst Site for takeoff operations

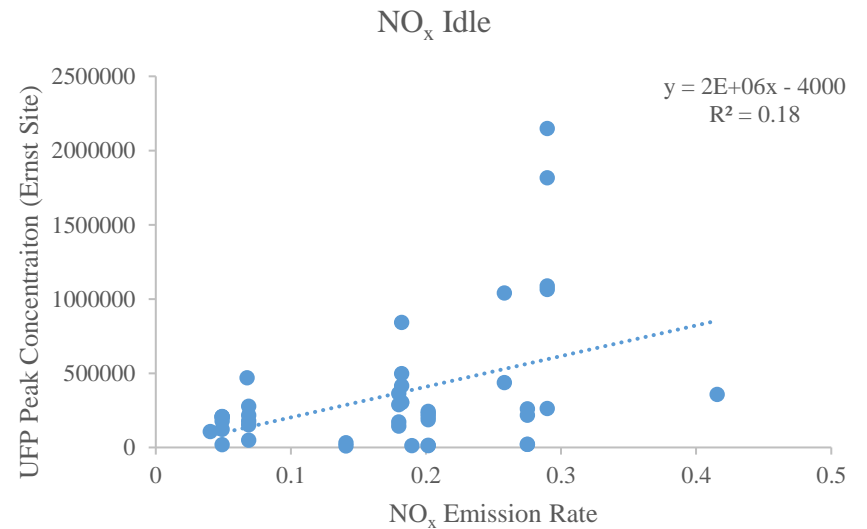
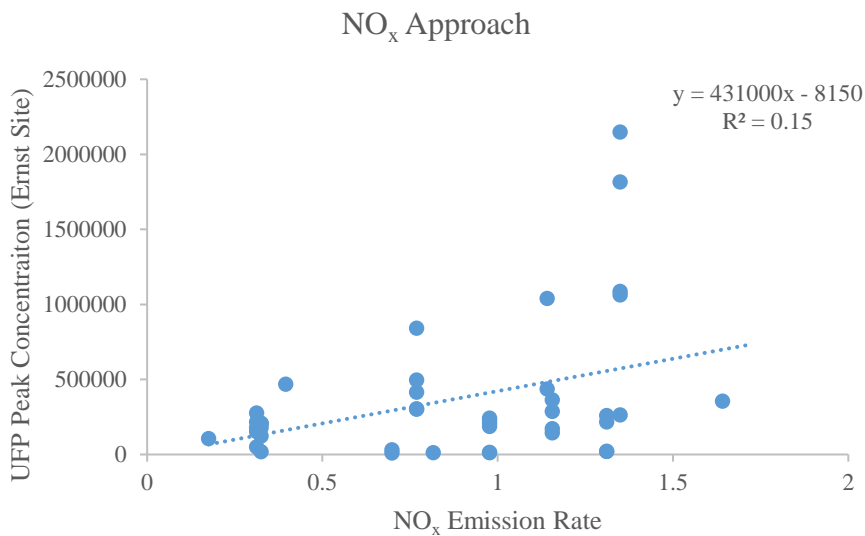
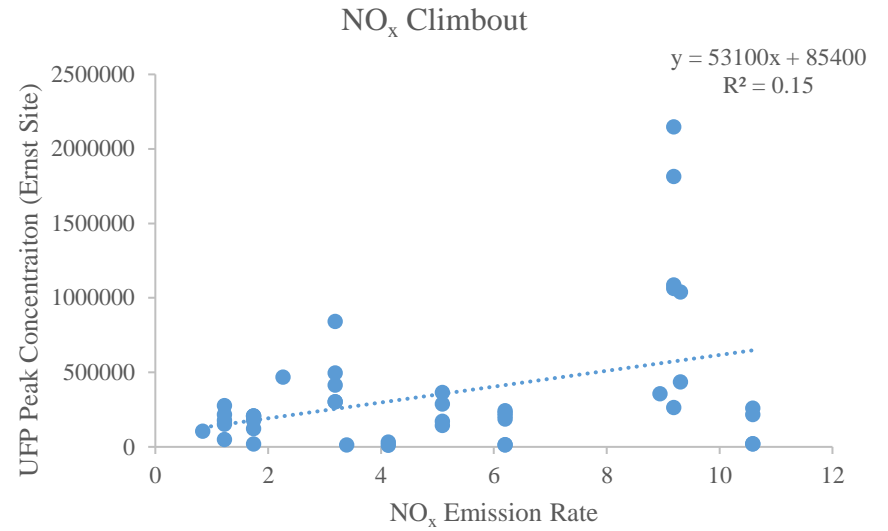
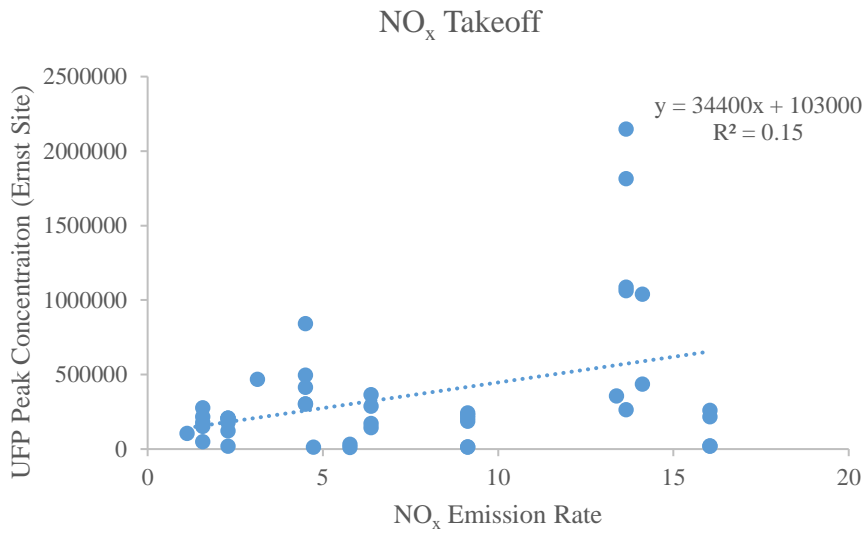


Figure 4. NO<sub>x</sub> emission rates for LTO cycle and UFP peak concentrations at the Ernst Site for takeoff operations

CO was significant for takeoff and climbout operating modes, which are at a higher thrust rating than idle and approach. This differs from what other studies have found. Schurmann et al. (2007) reported higher CO emissions at lower thrust settings, such as taxiing and idling, due to incomplete combustion of fuel. SN was significant for takeoff, approach, and idle with negative coefficients for all regressions. Previous studies (Stettler et al., 2012) described the use of smoke number as the current regulatory measure of aircraft particulate matter emissions and can quantify plume visibility. However, UFP do not fall in this size range. Very small particles may contribute substantially to light absorption but not scatter (Seinfeld, 1986). Landing operations were not significant for any of the ICAO parameters tested.

Use of ICAO database parameters to help determine UFP peak concentrations provides significant relationships, specifically for NO<sub>x</sub> and thrust, with thrust as the strongest predictor for UFP concentrations.

### *3.4 Engine Age*

Figs. 6 and 7 show the UFP peak concentration by engine age for the RW and Ernst sites, respectively. All engines with vintage information in the FAA N-Number database were included in the engine age analysis (231 takeoffs and 233 landings). The average aircraft vintage in the study for takeoff and landing was 2000. Aircraft built prior to versus after 2000 showed no significant difference in UFP peak concentrations (tested at  $p < 0.05$ ). This is in contrast to findings by Lobo et al. (2012) who measured PM emissions at Oakland Airport from idle/taxi and takeoff between 100 and 300 meters downwind, respectively. Lobo et al. (2012) found that older technology engines had as much as 3 times higher mass-based emission indices at takeoff compared with newer technology engines. However, the study does not compare older vs. newer

engines of the same make and model. Few studies have reviewed the difference between older and newer engines and UFP emissions.

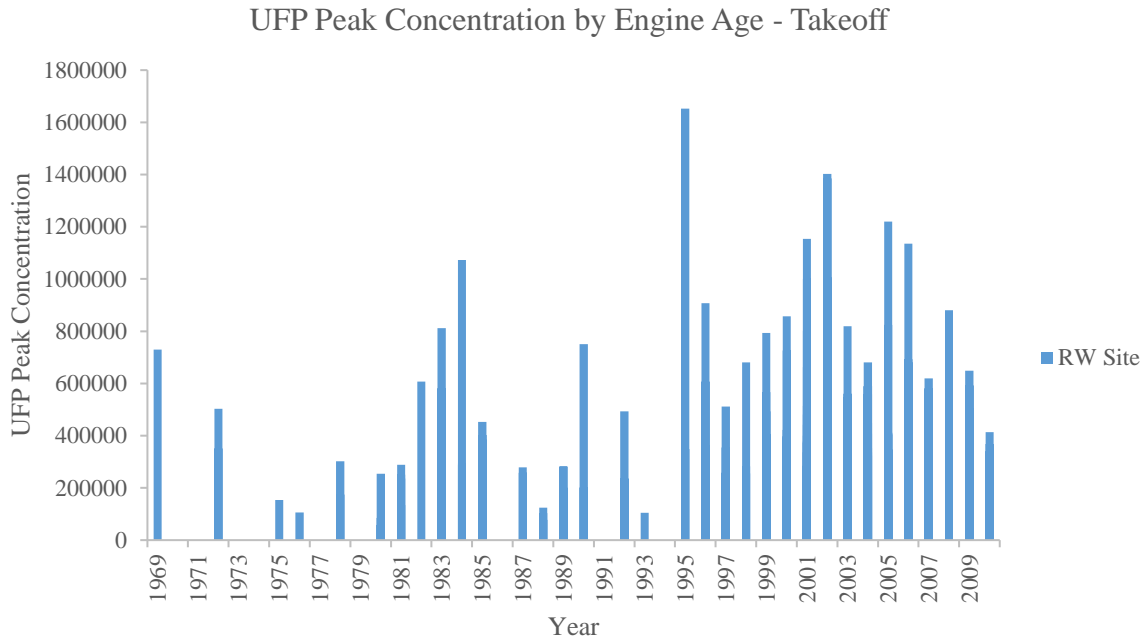


Figure 5. UFP peak concentrations compared to engine age for departures at the RW site



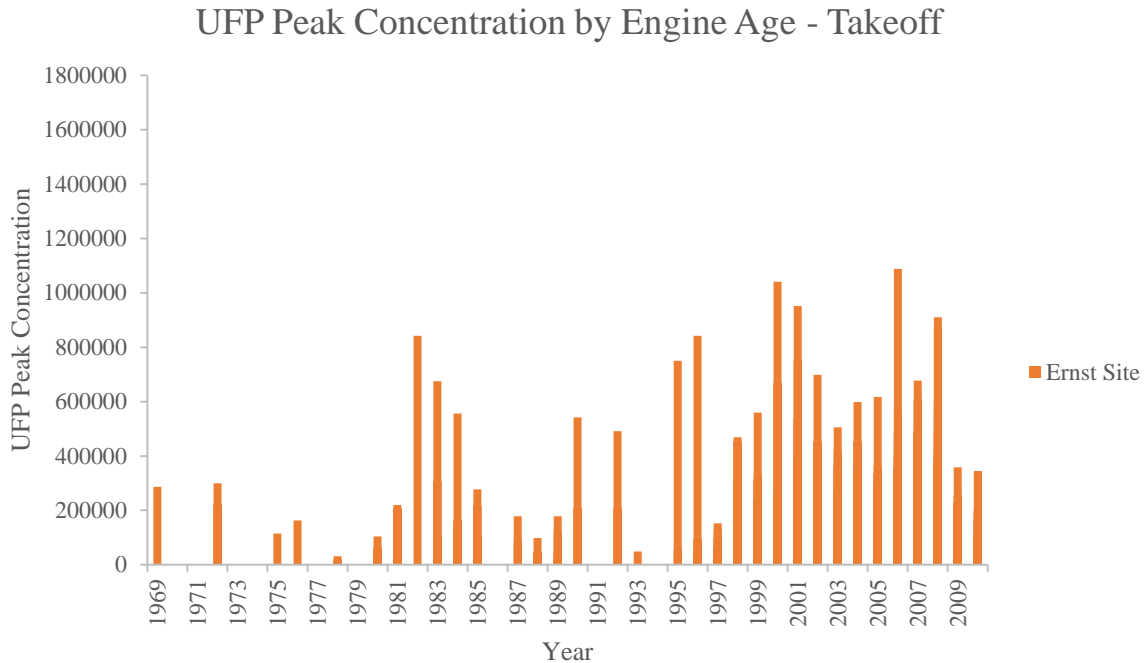


Figure 6. UFP peak concentrations compared to engine age for departures at the Ernst site

Similarly, for arrivals or all operations together, there was no significant dependence on engine age for pre/post 2000 engines.

UFP concentrations were then normalized by thrust and arrivals and departures were compared by site (Ernst and RW sites). The average engine vintage for this data set (for which we have thrust data) was 2002 for both takeoffs and landings. No significant dependence on engine vintage for UFP peak concentrations normalized by thrust was found.

#### 4. Conclusions and Recommendations

Few studies have examined UFP concentrations from landing operations (Hsu et al., 2014; Keuken et al., 2015; Hudda and Fruin, 2016). For data provided by SCAQMD for the SMO airport, we were able to assign specific peak UFP concentrations for both takeoff and landing operations with takeoff peak UFP concentrations significantly higher than landing. Per the ICAO database, engines operate at 100 percent thrust in takeoff mode and only 30 percent thrust in landing mode.

Higher thrust is needed to accelerate quite rapidly in takeoff mode, while during landing the aircraft is cruising in approach mode at a lower thrust rating. In a real-world setting, aircraft do not often operate at maximum thrust for departures to conserve fuel. Other studies have found that as an aircraft's landing trajectory is slower and longer, the impact area can be much larger (Hudda et al., 2014; Hudda and Fruin 2016).

It is important to understand the magnitude of UFP concentrations measured downwind from airports, especially because many neighborhoods are in close proximity to the airport. The data from the SMO airport study provided both takeoff and landing information for 370 and 374 operations, respectively. Using single variable linear regressions analysis showed that using ICAO database parameters to predict UFP peak measurements is best made by using thrust (kN) and NO<sub>x</sub>. Additional review of takeoff and landing operations at SMO for aircraft with engine information available in the ICAO database and corresponding UFP peaks could provide further information on the use of the ICAO database in predicting UFP from aircraft engines.

## Appendix

### *Airport Closure*

SMO was closed from September 19 – 24, 2010 presenting a natural experiment to measure UFP concentrations before, during, and after closure. Table A1 includes the average UFP measurements for the period prior to, during, and after the repaving and closure of the airport. These values are similar to those reported by the SCAMQD study, with the SCAQMD including additional days for the before and after averages (SCAQMD, 2011). The results are also in agreement with Hu et al. (2009), who also measured lower UFP concentrations during lower aircraft activity at SMO with concentrations sometimes dropping to the background level of 5,000  $\text{cm}^{-3}$ . Additionally, Choi et al. (2013) reported elevated UFP concentrations around SMO during the I-405 freeway closure, which resulted in decreased UFP concentrations in other sampling locations not next to the airport. Concentrations of UFP measured prior to and after repaving were significantly higher than during repaving. Additionally, average UFP concentrations taken at the Ernst Site prior to repaving were 15 percent higher than those taken after repaving (Table A1).

**Table A1: Average UFP Measurements Before, During, and After Repaving Project**

<b>Time Period</b>	<b>Average UFP at RW Site</b>	<b>Average UFP at Ernst Site</b>	<b>Takeoff Operation Counts</b>	<b>Landing Operation Counts</b>
Before Repaving (9/12/10 7:00 – 9/19/10 21:59)	25,700 ± 63,400	21,900 ± 42,600	152	152
During Repaving (9/19/10 22:00 – 9/24/10 7:59)	12,600 ± 11,100	11,300 ± 8,950	0	0
After Repaving (9/24/10 8:00 – 10/3/10 23:59)	28,800 ± 78,500	25,800 ± 61,600	219	222

*Multiple Operations for Single Aircraft*

During the study season, some aircraft took off and landed repeatedly, and their assigned peaks varied widely by factors of 3 – 12 for takeoff and 1 – 10 for landing (SI). Table A2 shows the range in UFP peak concentrations for the specific aircraft with multiple operations as well as the number of takeoffs and landings per specific aircraft for the study period. Fig. A1 shows the UFP peak concentrations assigned to each arrival and departure for the same aircraft by time of day.

**Table A2. Range in UFP Peak Concentration for Arrivals and Departures by Aircraft**

<b>AIRCRAFT REGISTRATION</b>	<b>ARRIVAL MINIMUM</b>	<b>ARRIVAL MAXIMUM</b>	<b>DEPARTURE MINIMUM</b>	<b>DEPARTURE MAXIMUM</b>	<b>SAMPLE SIZE</b>
<b>N969WR</b>	45,700	347,000	118,000	677,000	4 Arrivals & Departures
<b>N417C</b>	24,000	193,000	100,000	344,000	4 Arrival 5 Departures
<b>N311AF</b>	81,300	85,100	22,800	277,000	2 Arrivals 3 Departures
<b>N708GP</b>	84,600	355,000	32,700	419,000	8 Arrivals & Departures
<b>N7UF</b>	15,700	164,000	21,100	260,000	4 Arrivals & Departures

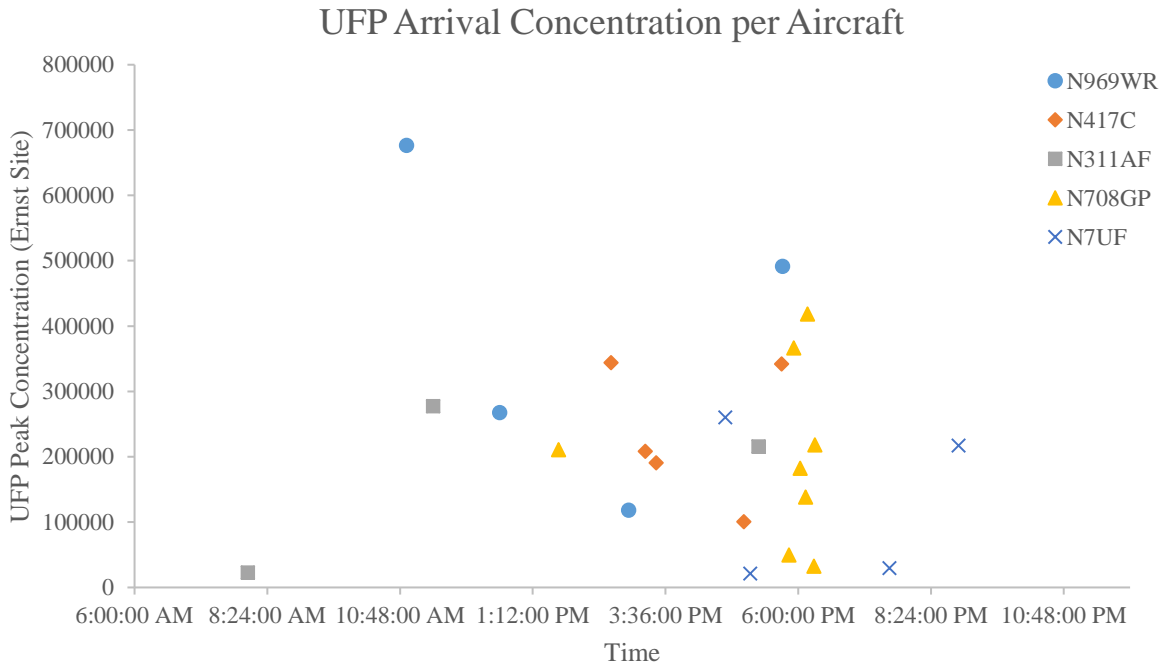
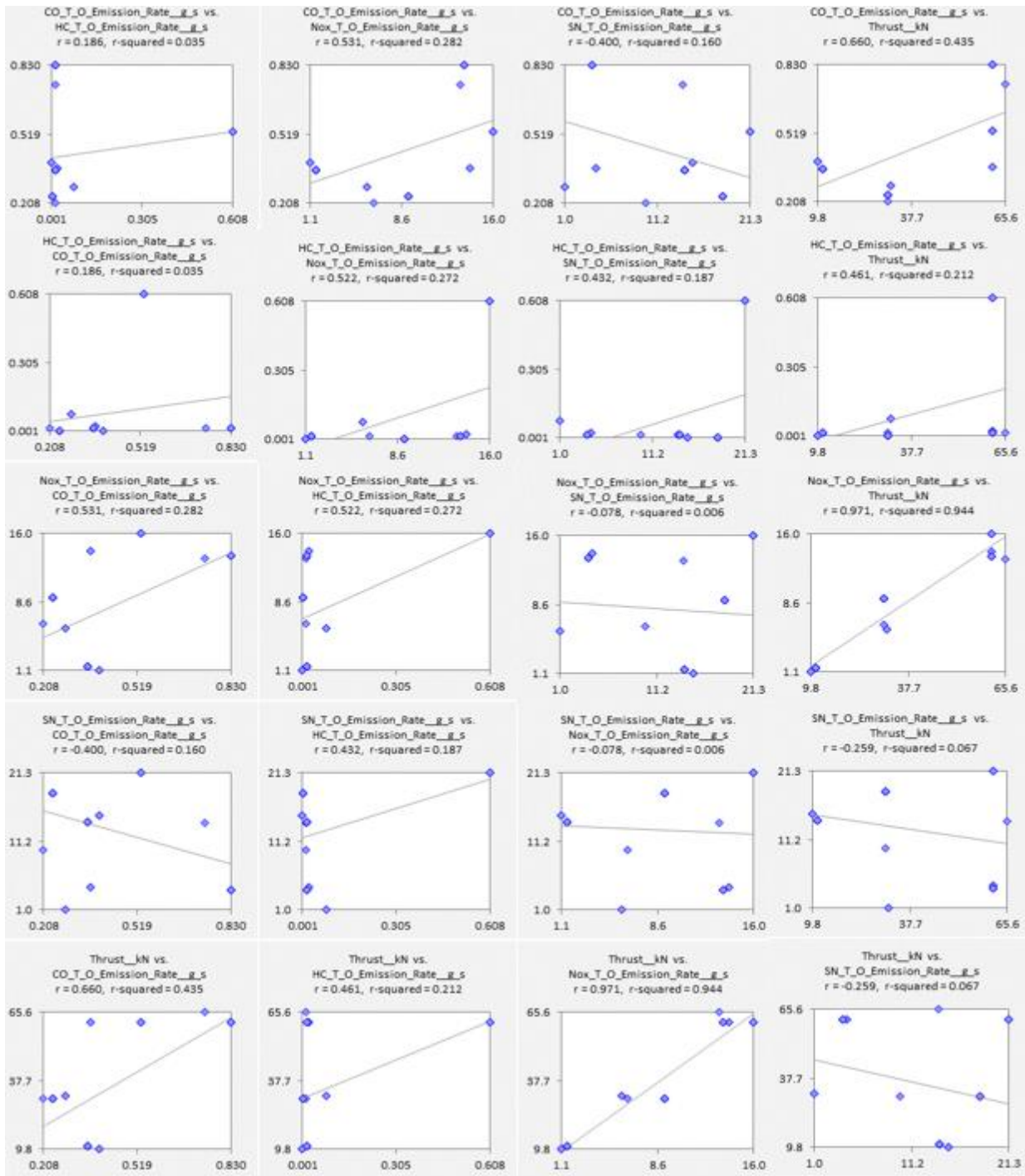


Figure A1. UFP peak concentrations for arrival operations per aircraft. Aircraft are identified by registration number.

Correlations between ICAO parameters for aircraft takeoff were plotted to determine relationship between variables (Fig. A2). Additionally, analyses included a correlation matrix for takeoff, approach, climbout, and idle.  $\text{NO}_x$  and thrust were highly correlated ( $R^2 = 0.94$ ). Data for other variables, including HC, CO, and SN were too small to determine significant correlation.



Variable	CO <sub>2</sub> T <sub>O</sub> Emission Rate <sub>g_s</sub>	HC T <sub>O</sub> Emission Rate <sub>g_s</sub>	NOx T <sub>O</sub> Emission Rate <sub>g_s</sub>	SN T <sub>O</sub> Emission Rate <sub>g_s</sub>	Thrust <sub>kN</sub>
CO <sub>2</sub> T <sub>O</sub> Emission Rate <sub>g_s</sub>	1.000				
HC T <sub>O</sub> Emission Rate <sub>g_s</sub>	0.186	1.000			
NOx T <sub>O</sub> Emission Rate <sub>g_s</sub>	0.531	0.522	1.000		
SN T <sub>O</sub> Emission Rate <sub>g_s</sub>	-0.400	0.432	-0.078	1.000	
Thrust <sub>kN</sub>	0.660	0.461	0.971	-0.259	1.000

Figure A2. Scatterplots and correlation matrix for correlations between NO<sub>x</sub>, HC, CO, SN, and thrust for takeoff emissions rates for takeoff operations.

## References

- Agrawal H, Sawant AA, Jansen K, Wayne Miller, J., Cocker III, D.R., 2008. Characterization of chemical and particulate emissions from aircraft engines. *Atmospheric Environment* 42, 4380-4392.
- Chalupa DC, Morrow PE, Oberdorster G, Utell MJ, and MW Frampton. 2004. Ultrafine deposition in subjects with asthma. *Environ Health Perspect.* 112(8): 879-882.
- Choi W, Hu S, He M, Kozawa K, Mara S, Winer AM, and SE Paulson. 2013. Neighborhood-scale air quality impacts of emissions from motor vehicles and aircraft. *Atmospheric Environment.* 80: 310-321.
- Delfino RJ, Sioutas C, and S Malik. 2005. Potential Role of Ultrafine Particles in Associations between Airborne Particle Mass and Cardiovascular Health. *Environ. Health Perspect.* 113(8): 934-946.
- Federal Aviation Administration. N-Number Registry. Accessed from: [http://registry.faa.gov/aircraftinquiry/NNum\\_Inquiry.aspx](http://registry.faa.gov/aircraftinquiry/NNum_Inquiry.aspx)
- Gong Jr. H, Linn WS, Clark KW, Anderson KR, Sioutas C, Alexis NE, Cascio WE, and RB Devlin. 2008. Exposures of Healthy and Asthmatic Volunteers to Concentrated Ambient Ultrafine Particles in Los Angeles. *Inhalation Toxicology.* 20(6): 533-545.
- Herndon SC, Onasch TB, Frank BP, Marr LC, Jayne JT, Canagaratna MR, Grygas J, Lanni T, Anderson BE, Worsnop D, and RC Mlake-Lye. 2005. Particulate emissions from in-use commercial aircraft. *Aerosol Sci. Technol.* 39: 799-809.
- Hoek G, Boogaard H, Knol A, De Hartog J, Slottje P, Ayres JG, Borm P, Brunekreef B, Donaldson K, Forastiere F, Holgate S, Kreyling WG, Nemery B, Pekkanen J, Stone V, Wichmann HE,

- and J Van Der Sliujs. 2010. Concentration response functions for ultrafine particles and all-cause mortality and hospital admissions: Results of a European expert panel elicitation. *Environ. Sci and Technol.* 44(1): 476-482.
- Hsu HH, Adamkiewicz G, Houseman EA, Spengler JD, and JI Levy. 2014. Using mobile monitoring to characterize roadway and aircraft contributions to ultrafine particle concentrations near a mid-sized airport. *Atmospheric Environment.* 89: 688-695.
- Hsu HH, Adamkiewicz G, Houseman EA, Vallarino J, Melly SJ, Wayson RL, Spengler JD, and JI Levy. 2012. The relationship between aviation activities and ultrafine particulate matter concentrations near a mid-sized airport. *Atmospheric Environment.* 50: 328-337.
- Hu S, Fruin S, Kozawa K, Mara S, Winer AM, and SE Paulson. 2009. Aircraft Emission Impacts in a Neighborhood Adjacent to a General Aviation Airport in Southern California. *Environ. Sci. Technol.* 43. 8039-8045.
- Hudda N and SA Fruin. 2016. International Airport Impacts to Air Quality: Size and Related Properties of Large Increases in Ultrafine Particle Number. *Environ. Sci. Technol.* 50. 3362-3370.
- Hudda N, Gould T, Hartin K, Larson TV, and S Fruin. 2014. Emissions from an International Airport Increase Particle Number Concentrations 4-fold at 10 km downwind. *Environ. Sci. Technol.* 48. 6628-6635.
- International Civil Aviation Organization. 2018. ICAO Aircraft Engine Emissions Databanks. Accessed from: <https://www.easa.europa.eu/easa-and-you/environment/icao-aircraft-engine-emissions-databank>



- International Civil Aviation Organization. 2012. Airport Air Quality Manual. Doc 9889 First Edition Corrigendum No. 1.
- Keuken MP, Moerman M, Zandveld P, Henzing JS, and G Hoek. 2015. Total and size-resolved particle number and black carbon concentrations in urban areas near Schiphol airport (the Netherlands). *Atmospheric Environment*. 104: 132-142.
- Kirchstetter TW, Harley RA, Kreisberg NM, and MR Stolzenburg. 1999. On-road measurement of fine particle and nitrogen oxide emissions from light- and heavy-duty motor vehicles. *Atmospheric Environment*. 33(18): 2955-2968.
- Lobo P, Hagen DE, and PD Whitefield. 2012. Measurements and analysis of aircraft engine PM emissions downwind of an active runway at the Oakland International Airport. *Atmospheric Environment*. 61: 114-123.
- Lobo P, Hagen DE, Whitefield PD, and DJ Aloes. 2007. Physical characterization of aerosol emissions from a commercial gas turbine engine. *J. Propul. Power*. 23: 919-929.
- Masiol M and RM Harrison. 2014. Aircraft engine exhaust emissions and other airport-related contributions to ambient air pollution: A review. *Atmospheric Environment*. 95: 409-455.
- Mazaheri M, Johnson GR, and L Morakawa. 2009. Particle and Gaseous Emissions from Commercial Aircraft at Each Stage of the Landing and Takeoff Cycle. *Environ. Sci. Technol*. 43. 441-446.
- Moore RH, Shook MA, Ziemba LD, DiGangi JP, Winstead EL, Rauch B, Jurkat T, Thornhill KL, Crosbie EC, Robinson C, Shingler TJ, and BE Anderson. 2017. Take-off engine particle emission indices for in-service aircraft at Los Angeles International Airport. *Scientific Data*. 4: 170198 doi: 10.10385/sdata.2017.198 (198)

- Oberdorster G. 2000. Pulmonary effects of inhaled ultrafine particles. *International Archives of Occupational and Environmental Health*. 74(1): 1-8.
- Peters A, Wichmann HE, Tuch T, Heinrich H, and J Heyder. 1997. Respiratory Effects Are Associated with the Number of Ultrafine Particles. *Am J Respir Crit Care Med*. 155: 1376-1383.
- Pietropaoli AP, Frampton MW, Hyde RW, Morrow PE, Oberdorster G, Cox C, Speers DM, Frasier LM, Chalupa DC, Huang L, and MJ Utell. 2004. Pulmonary Function, Diffusing Capacity, and Inflammation in Healthy and Asthmatic Subjects Exposure to Ultrafine Particles. *Inhal. Toxicol. Sup 1*: 59-72.
- Riley EA, Gould T, Hartin K, Fruin SA, Simpson CD, Yost MG, and T Larson. 2016. Ultrafine particle size as a tracer for aircraft turbine emissions. *Atmos Environ*. 139: 20-29. Doi: 10.10106/j.atmosenv.2016.05.016
- Santa Monica Airport. Frequently Asked Questions. 2017a. Accessed from: <https://www.smgov.net/Departments/Airport/News/FAQs.aspx>
- Santa Monica Airport. Santa Monica City Council Takes Next Step to Shorten the Runway at Santa Monica Airport and Adopts Resolution to Ensure Airport Closure. 2017b. Accessed from: [https://www.smgov.net/Departments/Airport/News/Airport\\_Closure.aspx](https://www.smgov.net/Departments/Airport/News/Airport_Closure.aspx)
- Schurmann G, Schafer K, Jahn C, Hoffman H, Bauerfeind M, Fleuti E, and B Rappengluck. 2007. The impact of NO<sub>x</sub>, CO, and VOC emissions on the air quality of Zurich airport. *Atmospheric Environment*. 41: 103-118.
- Seinfeld JH. 1986. *Atmospheric Chemistry and Physics of Air Pollution*. Wiley Interscience Publication. Chapter 7. Properties of Aerosols: Visibility Degradation. pp. 289-302.

- South Coast Air Quality Management District. 2011. General Aviation Airport Air Monitoring Study: Follow-up Monitoring Campaign at the Santa Monica Airport.
- Stettler MEJ, Swanson JJ, Barrett SRH, and AM Boies. 2012. Updated Correlation Between Aircraft Smoke Number and Black Carbon Concentration. *Aerosol Sci. and Technol.* 47(11): 1205-1214.
- TSI. Water-Based Condensation Particle Counter 3785 Specs. Accessed from: <http://www.tsi.com/water-based-condensation-particle-counter-3785/>
- Westerdahl D, Wang X, Pan X, and KM Zhang. 2009. Characterization of on-road vehicle emission factors and microenvironmental air quality in Beijing, China. *Atmospheric Environment.* 43: 697-705.
- Westerdahl D, Fruin SA, Fine PL, and Sioutas C. 2008. The Los Angeles International Airport as a source of ultrafine particles and other pollutants to nearby communities. *Atmospheric Environment.* 42: 3143-3155.
- Wey, C.C., Anderson, B.E., Hudgins, C., Wey, C., Li-Jones, X., Winstead, E., Thornhill, L.K., Lobo, P., Hagen, D., Whitefield, P., Yelvington, P.E., Herndon, S.C., Onasch, T.B., Miake-Lye, R.C., Wormhoudt, J., Knighton, W.B., Howard, R., Bryant, D., Corporan, E., Moses, C., Holve, D., Dodds, W., 2006. Aircraft Particle Emissions Experiment (APEX). NASA/TM-2006e214382, ARL-TR-3903. U.S. National Aeronautics and Space Administration, Glenn Research Center, Cleveland, OH. Available at: <http://gltrs.grc.nasa.gov>.

Wey, C.C., Anderson, B.E., Wey, C., Miake-Lye, R.C., Whitefield, P., Howard, R., 2007. Overview on the aircraft particle emissions Experiment. *Journal of Propulsion and Power* 23, 898e905.

Zhu Y, Fanning E, Yu RC, Zhang Q, and JR Froines. 2011. Aircraft emissions and local air quality impacts from takeoff activities at a large International Airport. *Atmospheric Environment*. 45: 6526-6533.

# **Impact of Los Angeles International Airport on UFP Concentrations at Two Downwind Sites: Analysis Using Wind Direction, Diurnal Patterns, and Operational Composition**

**Erica Alvarado<sup>1</sup> and Suzanne E. Paulson<sup>2</sup>**

1. *Air Quality Group. Tetra Tech, Inc. 3475 East Foothill Blvd., Pasadena, CA 91107*
2. *Department of Atmospheric and Oceanic Sciences, University of California Los Angeles, Los Angeles, CA 90095-1772, USA*

## **Abstract**

Aircraft emit large quantities of ultrafine particles (UFP), and have been suggested to impact air quality as far as several kilometers (km) downwind of airports. While a number of studies have provided evidence for the importance of landing operations on pollutant levels in communities downwind of airports, separating takeoff from landing operations is challenging. The Los Angeles Air Quality and Source Apportionment Study, which took place from January to March and July to August 2012, monitored 5.5 to 258 nm particle concentrations every three minutes at two community sites located between 1,600 and 2,000 m from the end of the runways at Los Angeles International Airport (LAX). The data recorded during the second season is the focus here. We analyzed relationships between particle concentrations and wind direction, time of day, and aircraft. We find concentrations of < 30 nm particles at both sites to have a large contribution from landing operations but not departures or nearby roadways when the sites are roughly downwind of one or both runways. Sub-30 nm particles were positively correlated to arrivals and usually negatively correlated with wind speed. These variables explain a large degree of variability of the data, resulting in  $R^2$  values  $> 0.63$ . Additionally, the diurnal patterns of small UFP at the site can be qualitatively explained by a combination of diurnal arrival data and diurnal meteorological conditions.

## 1. Introduction

One of the least understood aspects of aircraft emissions are ultrafine particles (UFP). While no health studies have been performed directly on UFP from aircraft, other studies suggest UFP are responsible for adverse health effects, with these effects increasing for smaller particle sizes (Peters et al., 1997; Oberdorster, 2000; Penttinen et al., 2001). A number of health-related studies report an increase in respiratory and cardiovascular morbidity and mortality with UFP exposure (Peters et al., 1997; Delfino et al., 2005; Hoek et al., 2010). Additionally, respiratory problems, specifically asthma and its symptoms, are exacerbated by UFP exposure (Chalupa et al., 2004; Pietropaoli et al., 2004; Gong et al., 2008).

Additional emissions from aircraft include nitrogen oxides (NO<sub>x</sub>), black carbon (BC), carbon monoxide (CO), sulfur (S), and hydrocarbons (HCs). Elevated NO<sub>x</sub> emissions from aircraft have been measured up to 2.6 km from Heathrow airport (Carlaw et al., 2006). BC concentrations have also been found to be positively associated with takeoff and landing operations (Dodson et al., 2009; Hu et al., 2009a).

UFP from aircraft operations have been measured close to the airport as well as many km downwind (Westerdahl et al., 2008; Hu et al., 2009a; Zhu et al., 2011; Choi et al., 2013; Hsu et al., 2012; Hsu et al., 2013; Hudda et al., 2014; Hudda and Fruin, 2016). Hudda et al. (2014) measured a 2-fold increase in particle number concentrations up to 16 km and a 4- to 5-fold increase between 8 and 10 km downwind of LAX, and attributed a portion of UFP collected attributed to arriving flights. At Schiphol Airport in the Netherlands, measurements collected downwind of the airport and supported by Gaussian plume models found UFP impacts over 8 km away from the airport (Keuken et al., 2015). The long distances at which UFP were detected are in sharp contrast to a number of studies that consistently show freeway plumes disappear

completely in 300 m and are typically > 90 percent dissipated in 100 m (Karner et al., 2010) during daytime and within approximately 2.5 km at night and during early morning (Choi et al., 2012; Choi et al., 2013).

As aircraft preferentially takeoff and land into the prevailing wind, the downwind area is typically both below the arrival path and downwind of the takeoff area, an arrangement that confounds separation of the impacts of landing versus takeoff operations. Particulate emissions from aircraft have been attributed to both takeoff and landing operations at multiple airports (Unal et al., 2005; Westerdahl et al., 2008; Hu et al., 2009a; Zhu et al., 2011; Hsu et al., 2012; 2013; 2014; Choi et al., 2013; Hudda et al., 2014; Keuken et al., 2015; Hudda and Fruin, 2016; Moore et al., 2017). The majority of this work has focused on takeoff operations, and multiple studies have found spikes in UFP number concentrations to correlate to takeoff operations. Zhu et al. (2011) were able to assign UFP spikes to specific takeoffs at 600 m downwind of the runway at LAX, and Westerdahl et al. (2008) measured a maximum peak of 4.8 million particles  $\text{cm}^{-3}$  100 m downwind of an LAX runway.

A number of studies have found evidence for landing operations on elevated UFP concentrations downwind of airports (Westerdahl et al., 2008; Hsu et al., 2014; Keuken et al., 2015; Hudda et al., 2014; Hudda and Fruin, 2016; Riley et al., 2016). Riley et al. (2016) measured a three- to five-fold increase over background particle emissions (defined as the measured concentrations 5<sup>th</sup> percentile) at 5 and 10 km under the aircraft landing path at both LAX and Hartsfield-Jackson International Airports. Hudda et al. (2014) found elevated particle numbers under landing jet trajectories during westerly winds at LAX airport with concentrations at 8 km downwind exceeding 75,000 particles  $\text{cm}^{-3}$  as compared to the measured urban background which ranged from 5,000 – 20,000 particles  $\text{cm}^{-3}$ , and 4-fold and 2-fold increases in particle number

concentrations over a baseline concentrations at 10 km and 16 km, respectively. Hudda and Fruin (2016) measured spikes in the numbers of ultrafine particles up to 2.75 km from LAX, under the landing path of aircraft. UFP from landing operations were also observed 500 m downwind of LAX, with UFP particle count peaks corresponding to individual aircraft landing operations (Westerdahl et al., 2008).

The peak median/mean of the UFP size distribution from aircraft measured in community settings consistently falls between 10-15 nm (Westerdahl et al., 2008; Hu et al., 2009a; Zhu et al., 2011; Lobo et al., 2012; Keuken et al., 2015), with ranges up to 18-25 nm. These size particles from aircraft are comprised of sizes smaller than on road emission sources, which range between 20-130 nm for diesel engines and 20-60 nm for gasoline engines (Morawska et al., 1998; Ristovski et al., 1998).

Here, we analyze the contribution of takeoff and landing operations on UFP concentrations at two community sites between 1,600 and 2,000 meters downwind of LAX. The farther site is also located approximately 450 meters east of the I-405 Freeway. We analyze concentrations of < 30 nm and 30-98 nm particles and their dependence on wind direction, time of day, and aircraft takeoff and landing operations to determine the impact of the airport operations at the two sites. We determine the contribution of arrivals and departures by runway, arrivals compared to departures, and diurnal UFP concentrations to overall UFP concentrations at the two community sites. The analysis allows us to clearly separate the contributions from takeoff versus landing operations.

## **2. Methods**

### *2.1 Sites*

The Los Angeles World Airports Phase III Air Quality and Source Apportionment Study (LAX AQSAS) used several sites, two of which were equipped to measure particle size distributions, the



Community North (CN) and Community East (CE) sites (Fig 1.) The CN site was located 1,651 and 1,658 meters from the ends of RW24 L (North [N]) and 24 R (N), respectively. The CE site was located 1,700 and 1,952 meters from the ends of RW25 R (South [S]) and 25 L (S), respectively. Collectively RW24 R/L (N) are known as the North Airfield and RW25 R/L (S) as the South Airfield. The North and South Airfields are approximately 1,600 m apart from one another, and are exactly parallel and aligned with the prevailing daytime wind. When operations switch to takeoff and landing to the east, runways are referred to as 06R/L and 07R/L (now shown).

## 2.2 *Data Set*

Data used here were collected during the LAX AQSAS Summer Season conducted from 7/18/2012 to 8/28/2012, for a total of 42 days. Due to instrument problems at the CN site, SMPS measurements were not collected from 8/8/2012 – 8/28/2012.

Scanning Mobility Particles Sizers (SMPS) SMPS 3936N25A (TSI Inc., Shoreview, MN) and SMPS 3936L10 at the CN and CE sites, respectively operated for 24 hours/day, collecting size distributions every 3 minutes. The scanning process means that the instrument only measures each of the < 30 nm and 30-98 nm size bins every 3 minutes, an arrangement that is not ideal for measurements of the transient peaks associated with aircraft operations. To address this limitation, we averaged UFP data into 30 minute bins, so that each measurement contains 10 “snapshot” measurements of these particle size bins of interest. Further discussion of SMPS measurements is included in the Appendix.

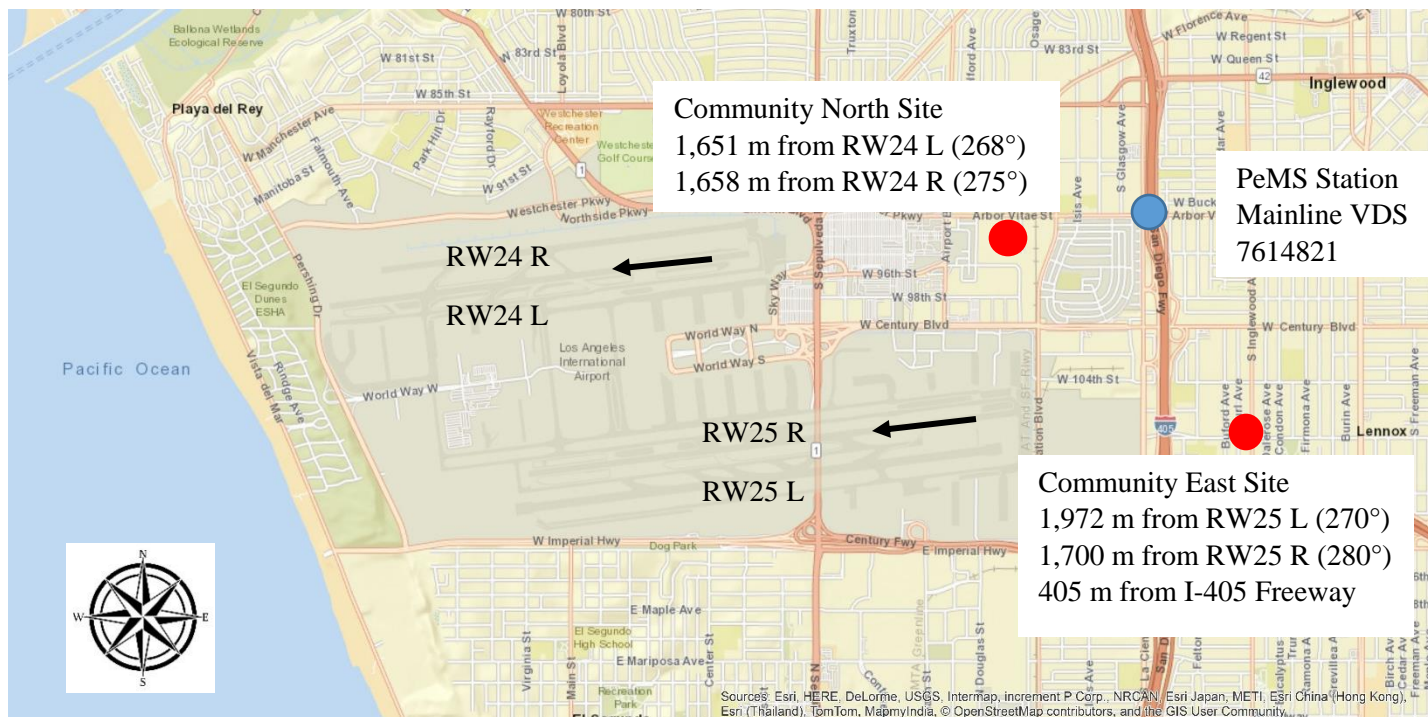


Figure 1. LAX AQSAS site locations (LAX AQSAS, 2013). The two sites used here are the Community North (CN) and Community East (CE) sites which are located downwind of the North and South Airfield runways, respectively. Predominant flight paths are shown with black arrows. The distance from each runway and the sites angle from the runway is included. An additional site included in the PeMS Station Mainline VDS 7614821 which is indicated in blue.

The range of particle sizes measured was 5.5 to 289 nm and 4.61 to 156 nm at the CE and CN sites, respectively. The SMPSs report particle counts by size bin (dN/dlogDp). Each bin is multiplied by dlogDp (TSI, 2010) and summed for the indicated size ranges (< 30 and 30-98 nm) used here.

A Met One Model 010 sensor installed on a 10-meter tower at the CE site collected one minute wind direction (WD) and wind speed (WS) data (LAX AQSAS, 2013). Figure 2 shows wind directions for the full six-week season; winds were consistent and predominantly from 250°, west/southwest (WSW) during the day. Measurements at the CE site for nighttime wind directions were recorded between the hours of 00:00 to 06:00. Winds were more variable during the early morning hours with the average direction approximately 240° between 00:00 to 06:00.

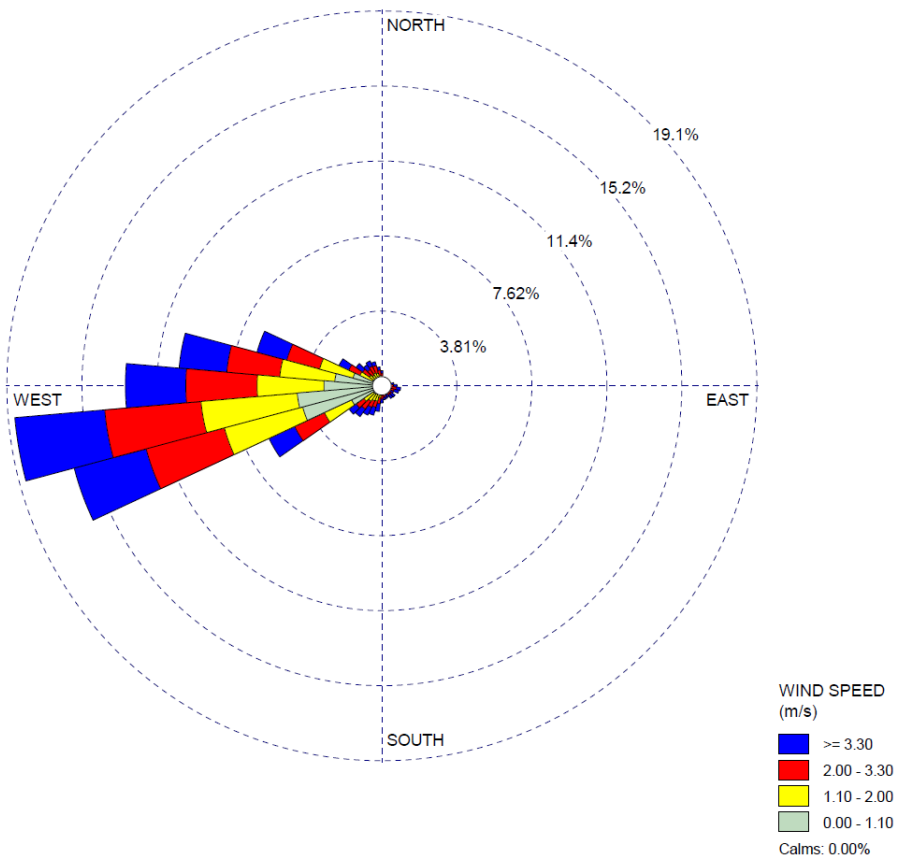


Figure 2: Wind rose plot for the Summer Season at the Community East site.

The average wind speed for the study season was 2.2 m/s, resulting in a transport time to the CE and CN sites from the end of the runway of approximately 12 minutes. UFP concentrations were time shifted by 12 minutes to account for the calculated transport time.

### 2.3 *LAX Operations*

Aircraft operation data obtained from Los Angeles World Airports included type of operation (arrival/departure), time of day, runway used, airline, aircraft type, operator, and flight tail number. A total of 69,792 operations took place during the study, with 98 percent taking place on RW24 (N) and 25 R/L (S) (taking off and landing to the west). Operations on RW06 and 07R/L (taking off and landing to the east) were primarily during the early morning hours to comply with noise reduction requirements at the airport (LAX, 2018). Only one percent of operations on RW06/07 during the study season were outside of the midnight to 06:00 window. Additionally, more arrivals occurred than departures during this timeframe. Discussion of number of arrivals and departures is found in the Appendix.

## **3. Results and Discussion**

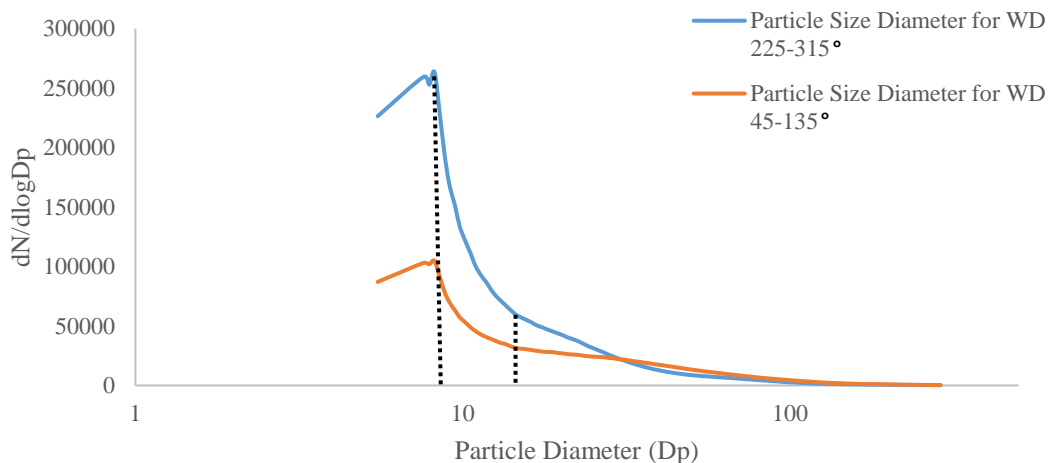
### 3.1 *General Features of UFP at the CE and CN Sites*

During conditions when airport operations are upwind of the sites, UFP measurements at the CE and CN site are dominated by smaller sized particles. Figure 3a shows size distributions for the CE site when the site is downwind and upwind of the airport. The number concentrations are higher for the smaller particle diameters when the CE site is downwind of airport operations as compared to conditions when the site is upwind. Figure 3b shows the number concentration size distribution for the CN site when the site is downwind and upwind of the airport, respectively. The CN site measurements are similar to the CE site with higher number concentrations of smaller particles when the site is downwind of the airport. As with other studies, there are higher counts of smaller sized particles with the number concentration decreasing with larger sized particles, particularly for the CE site which has a peak at the particle diameter of 8.2 nm both upwind and downwind of the airport as well as a much smaller peak at approximately 20 nm (Fig 3a). Both

peaks are indicated with a dotted line. Particle counts at the CN site are much lower for smaller sized particles than the CE site. Additionally, the CN site peak concentrations were at 17.5 and 21.7 nm when the site is downwind and upwind of the airport, respectively (Fig 3b). The peak concentration sizes are similar to several other studies measuring UFP from aircraft operations (Westerdahl et al., 2008; Hu et al., 2009a; Zhu et al., 2011; Lobo et al., 2012; Keuken et al., 2015).

Lobo et al. (2012) reported the geometric mean diameter for the PM number based emission index at takeoff to be  $13.2 \pm 5.3$  nm with a geometric standard deviation of  $1.58 \pm 0.32$ . Herndon et al. (2005), looking at particulate emission indices for takeoff and idle aircraft, measured a peak in particulate size distribution at or below the instrument cutoff of 30 nm and at approximately 90 nm. Here, we used a more conservative cutoff point of  $< 30$  nm compared to other studies which had finer resolution data (Westerdahl et al., 2008; Hu et al., 2009; Zhu et al., 2011; Choi et al., 2013) and did not use size bins, such as  $< 30$  and 30-98 nm. A Data Quality Statement on the Pittsburgh Air Quality Study, which used the two SMPS models used here, said the best precision is expected by the 3936L10 (used at the CE Site for this study) and the worst precision is expected by the 3936N25A (used at the CN Site for this study) which also sized particles 7% larger than the 3936L10 (Atmospheric Science Data Center, 2003). Additionally, multiple studies have used the 3936N25A to measure the smaller UFP while the 3936L10 was used to measure larger UFP sizes (Park et al., 2006) with Chow et al. (2006) classifying the 3936L10 as a fine particle SMPS and the 3936N25A as a nano-particle SMPS.

CE Site: Distribution of Particle Size Diameter 5.5-289 nm



CN Site: Distribution of Particle Size Diameter 5.5-157 nm

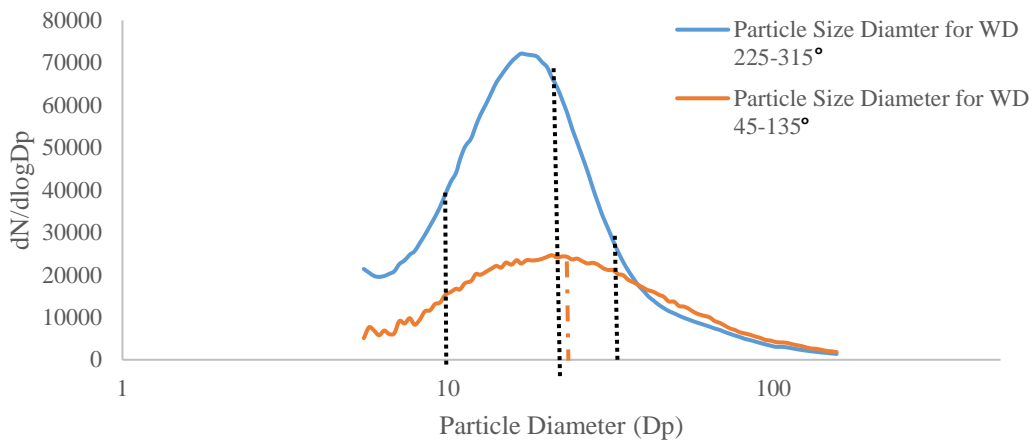


Figure 3a - b. (a) Particle number size distribution for CE site for wind directions placing site downwind at 225-315° and wind directions placing site upwind at 45-135°. Peaks are indicated with dotted lines. X-axis is on a log scale. (b) Particle number size distribution for CN site for wind directions placing site downwind at 225-315° and wind directions placing site upwind at 45-135°. Dotted line indicates peak for 225-315° and dashed line indicates peak for 45-135°. X-axis is on a log scale.

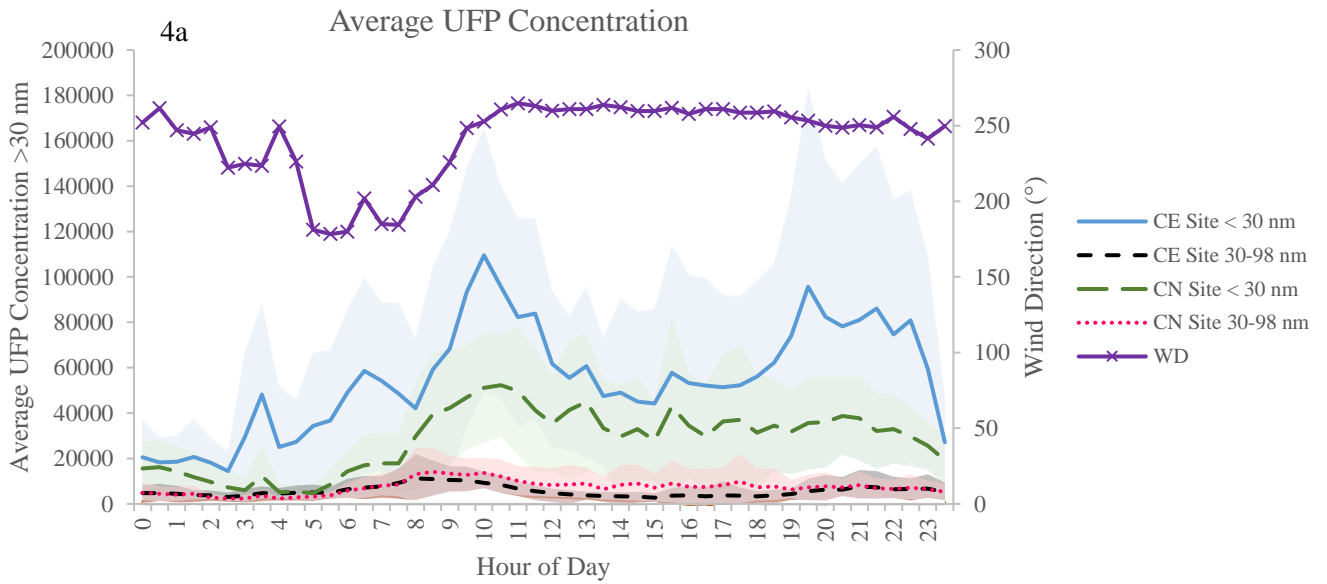
The general features of  $< 30$  nm UFP numbers at both sites are mostly explained by a combination of arrival operations and meteorology. At the CE site,  $< 30$  nm UFP have a pronounced peak at 10:00 and a broader peak from 19:30 – 22:30 (Fig 4a). The morning peak

roughly corresponds to a local peak in arrival activity around that time (Fig 4b). Both departures and arrivals increase steeply beginning around 06:00, but at this time, the wind direction is blowing roughly from the sampling sites toward the airport. As the morning progresses, the average wind direction becomes progressively more optimal for the CE site, reaching about  $290 - 10^\circ$  until around 11:00 when it stabilizes at  $250 - 260^\circ$ . Arrivals are fairly constant from approximately 13:00 – 19:00, yet this period experiences much lower UFP concentrations. This period also corresponds to somewhat higher wind speeds, which have been observed to increase dispersion and lower pollutant concentrations (Choi et al., 2016). The afternoon UFP peak corresponds to a period when wind speeds begin to drop somewhat and when arrivals spike again. They remain high for a few hours, even though arrivals have dropped off, possibly because wind speeds drop dramatically after this time. The CN site has a similar but weaker pattern (Fig 4a). Additionally, the UFP peaks measured at the CE and CN sites do not follow the traffic patterns observed on the I-405 freeway around LAX.

The pattern for 30-98 nm particles has much less diurnal variation, reading a slight peak somewhat earlier than the  $< 30$  nm UFP (Fig 4a). Unlike the  $< 30$  nm UFP, which are nearly twice as high at the CE vs. CN site ( $55,000$  vs.  $28,100$  particles  $\text{cm}^{-3}$ , respectively) the 30-98 nm particles are slightly higher at the CN site ( $p=0.002$ ).

Figure 4a shows the average UFP concentrations  $< 30$  nm and 30-98 nm for the CE and CN sites as well as the average wind direction versus time of day. UFP concentrations of  $< 30$  nm and 30-98 nm size bins were averaged in half-hour bins for the CE and CN sites. Also shown are the  $\pm$  standard deviation bands for all values, the half-hour averaged departure and arrival data and traffic data, and bands indicating when the airport is downwind. The diurnal pattern is mostly explained by a combination of wind direction, speed, and aircraft arrival activity.

Figure 4b shows total arrivals per runway and wind speeds per half hour. Figure 4c shows the average diurnal traffic pattern at a Performance Measurement System (PeMS) station (CalTrans, 2018) located on the I-405 freeway approximately 2.5 km east of the end of the North Airfield and approximately 450 m east of the CN site. Total aircraft departures are also included for comparison. A figure showing flight paths can be found in Fig 1.





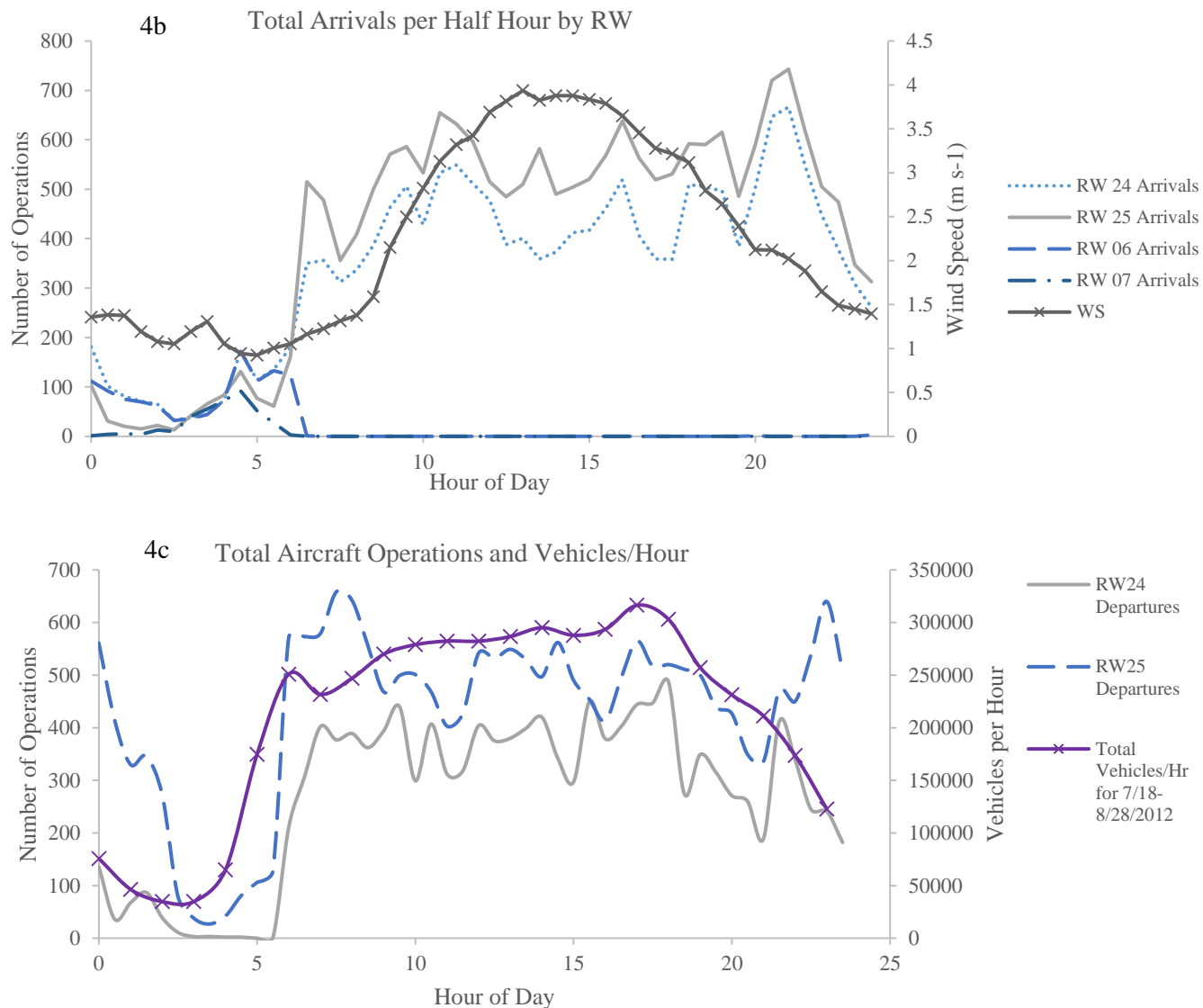


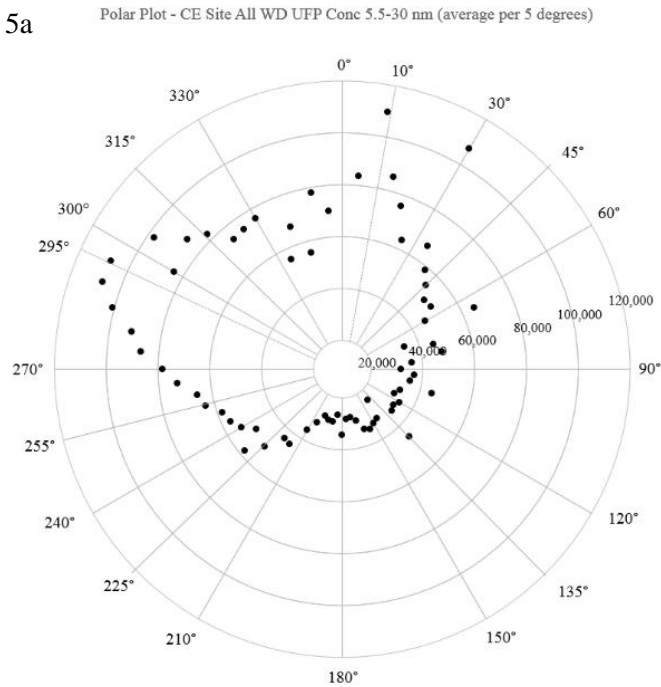
Figure 4a - c. (a) Diurnal half-hour averages for the entire study season for UFP concentrations < 30 and 30 – 98 nm at the CE and CN sites for RW24/25 compared with (b) Arrivals operational counts by runway and average wind speed. Runways 24 and 25 indicate operations to and from the west and Runways 06 and 07 indicate operations to and from the east. (c) Total vehicles per hour for 7/18-8/28/2012 and total departures operational counts by runway.

Figure 5a shows the UFP concentrations for < 30 nm averaged for each 5° wind direction bins for the CE site, for times when operations were on RW24 (N) and 25 (S). The plot shows low concentrations (mostly approximately 14,000 cm<sup>-3</sup>) for wind directions between 60° and 210°.

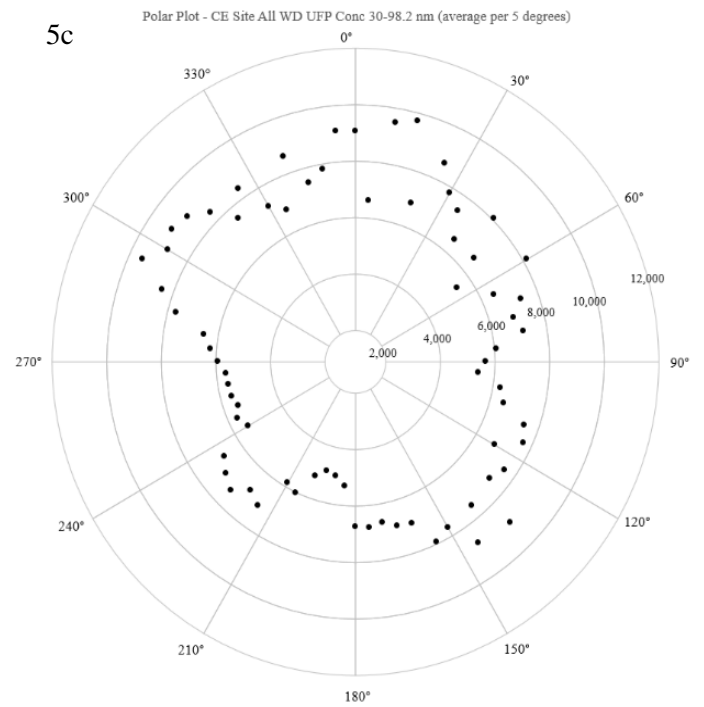
Concentrations increase rapidly from 210° to 290°, where they peak at 108,000 cm<sup>-3</sup>, and then decrease to approximately 72,000 cm<sup>-3</sup> at approximately 340°, and increase again to approximately 108,000 cm<sup>-3</sup> at 10° and then drop down again. While concentrations are elevated at 270°, the direction of both the closest runways (25R/L [S]) and the I-405 freeway, there is no peak indicating a source at 270°, instead concentrations increase continuously to 290°. The wind direction dependence of concentrations are much more consistent with a dominant contribution from landing operations, particularly on the North Airfield (RW24 R/L [N]).

Figure 5b shows average < 30 nm UFP concentrations for each 5° wind direction bin for the CN site. This plot shows the lowest concentrations (approximately 13,700 cm<sup>-3</sup>) for wind directions between 310° and 120°, with some smaller peaks at 345° and 25° (approximately 25,000 and 27,000 cm<sup>-3</sup>, respectively). The concentrations increase rapidly between 120° and 190°, peaking at 30,000 cm<sup>-3</sup> and increase again between 190° and 310° to approximately 46,000 cm<sup>-3</sup>. The closest runways are located between 268° and 275°, close to the direction of the peak concentrations. Similar to the CE site, the pattern is consistent with landing operations passing over the monitoring site prior to touching down on the North Airfield runways (24R/L), together with a contribution from landing operations on the South Airfield.

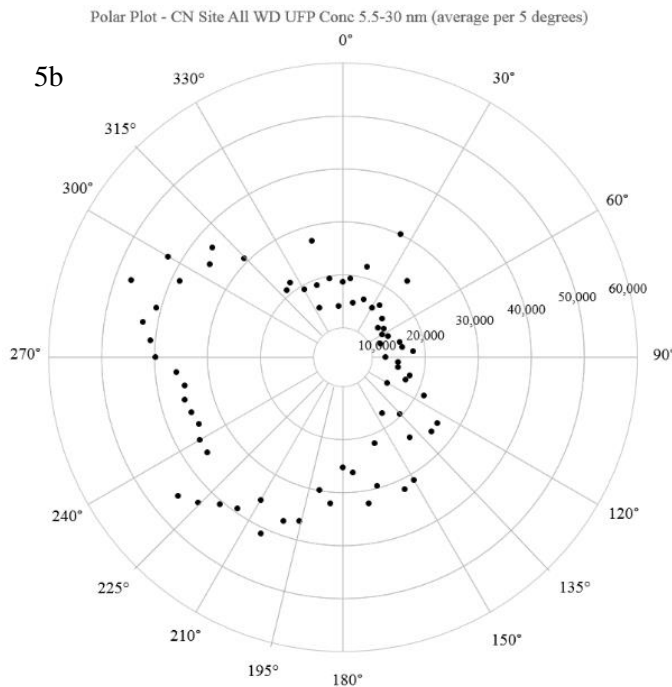
5a



5c



5b



5d

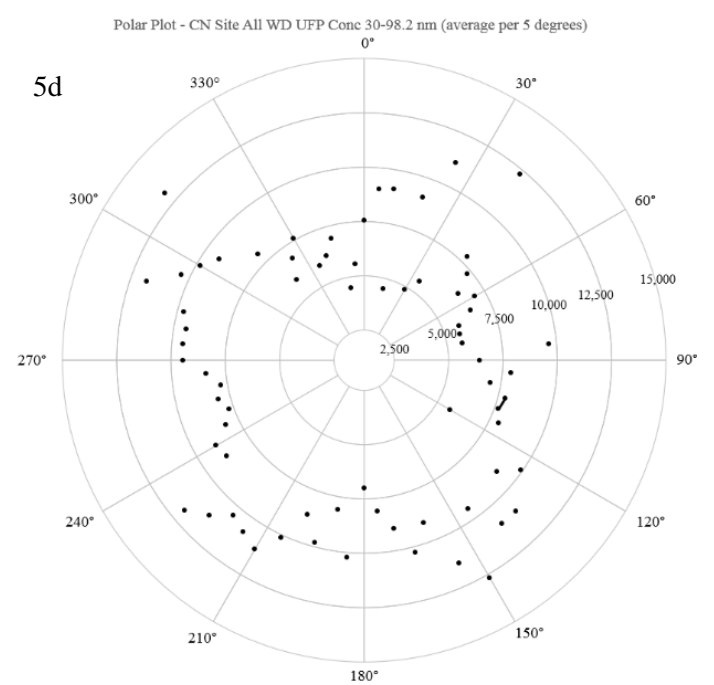


Figure 5a-d. Polar plots of UFP concentrations by all wind directions for aircraft operations on RW24/25 at the (a) CE site for < 30 nm; (b) CN site for < 30 nm; (c) CE site for 30-98 nm; and (d) CN site for 30-98 nm. Axes are for a and b are set to (a) 120,000 and (b) 60,000. Axes for c and d are set to (c) 12,000 and (d) 15,000. The majority of UFP concentrations were from the northwest for the < 30 nm sized particles at the CE site (a) and from the west/northwest at the CN site (b).

Figures 5c and 5d show 30-98 nm UFP concentrations averaged for 5° wind direction bins for the CE and CN sites, respectively. The 30-98 nm plots show no clear peaks, in contrast to the plots of < 30 nm UFP concentrations at the CE and CN sites (Figures 5a and 5b, respectively). Figure 5c shows concentrations slightly lower for winds from the west/southwest (240° to 270°) when the CE site is downwind of the airport. At both sites, concentrations were mostly uniform for all wind directions for the 30-98 nm plots. For both sites, the average concentrations for 30-98 nm vary by only about factors of 60% to a factor of 2. Sub-30 nm particle concentrations vary by factors of 3-4, depending on wind direction.

### 3.2 *Multivariate linear regression*

Results of a multivariate linear regression of < 30 nm UFP, aircraft departures and arrivals on each runway, and wind speed averaged for 60° wind directions and 30-minute time bins are shown in Figures 6 and 7. Data were averaged over 30 minutes so that each bin included 10 SMPS runs. As each SMPS run lasts three minutes and only samples the smallest several bins for a fraction of each 3-minute window, and as operations are not evenly distributed but tend to cluster, 30 minute averages were chosen to provide more representative values and reduce random noise. To address multicollinearity, variables with both variance inflation factors (VIFs) greater than 5 and correlations greater than  $\pm 0.5$  were removed one at a time and the regression rerun separately for the correlated variables. In almost all cases, the VIF test resulted in removal of either RW24 (N) or RW25 (S) departures. Departures tend to be highly correlated with each other, and the multivariate regression typically cannot differentiate between the two runways. The result with the highest adjusted  $R^2$  value was used. Only variables with p-values < 0.05 are included in the final regressions. RW06/07, as well as wind directions from the north (345-360°; 0-45°) were also excluded due to low sample sizes.

Table 1 shows the regression results for the CE site by wind direction including the coefficients, the corresponding p-values, adjusted R<sup>2</sup> values, and sample sizes. Blanks in the table are for variables removed from the regression due to correlation effects.

For the CE site, arrivals are the most important predictor overall. For winds from the west and northwest (225-285° and 285-345°), arrivals on both RW24 (N) and 25 (S) are significant. For winds from the north and southwest, only arrivals on RW25 (S) are significant. When winds are from the east, the regression is consistent with no impacts from the airport at the site. The findings shown here are in agreement with those reported by Riley et al. (2016) and Hudda and Fruin (2016) who observed elevated smaller UFP between 800 m to 10 km downwind of LAX and attributed these concentrations to landing operations. In all cases, except all wind directions together, particles < 30 nm were strongly inversely related to the wind speed, as is expected due to the association of higher wind speed and higher atmospheric dispersion.

**Table 1: Regression Coefficients and p-values for CE Site UFP Concentrations < 30 nm**

<b>CE SITE &lt;30 NM</b>	<b>ALL WD</b>	<b>225°-285°</b>	<b>285° -345°</b>	<b>45° -105°</b>	<b>105° -165°</b>	<b>165° -225°</b>
<b>Sample Size</b>	<b>1,781</b>	<b>1,230</b>	<b>191</b>	<b>57</b>	<b>103</b>	<b>108</b>
<b>Constant</b>	28,900***	40,100***	-481	43,500***	27,100*	23,900***
<b>coeff.</b>						
<b>p-value</b>	(0.00)	(0.00)	(0.955)	(0.00)	(0.00)	(0.00)
<b>RW24 (N) Arrival</b>	2,030*	2,140***	4,470***			-1,110
	(0.00)	(0.00)	(0.00)			(0.20)
<b>RW24 (N) Departure</b>	280	366	-620	2,470	1,020	-516
	(0.48)	(0.87)	(0.60)	(0.20)	(0.28)	(0.53)
<b>RW25 (S) Arrival</b>	1,630*	1,360**	4,800***	4,160**	446	2,070**
	(0.00)	(0.01)	(0.00)	(0.01)	(0.55)	(0.01)
<b>RW25 (S) Departure</b>	-228	530		-39.1	999	674
	(0.50)	(0.24)		(0.97)	(0.06)	(0.24)
<b>Wind Speed</b>	-2,240	-7,710***	16,900**	-35,800***	-20,400***	-11,100*
	(0.08)	(0.00)	(0.01)	(0.00)	(0.00)	(0.03)
<b>Adjusted R<sup>2</sup></b>	0.10	0.06	0.63	0.41	0.20	0.05

\*p<0.05, \*\*p<0.01, \*\*\*p<0.001

UFP concentrations measured for winds from the northwest (Fig 6) had the highest adjusted  $R^2$  value and provided the best fit, with the expressions (all variables significant).

$$\text{Predicted UFP} = -911 + 4,270 \text{ RW24 A} + 4,639 \text{ RW25 A} + 16,753 \text{ WS}$$

Average values were 18,800, 25,500, and 21,800 for RW24 (N) arrivals, RW25 (S) arrivals and wind speed, indicating that the importance of the variables is approximately RW25 (S) arrivals, wind speed, and RW24 (N) arrivals. Plots for additional wind directions of actual versus predicted < 30 nm UFP concentrations can be found in the Appendix.

Regressions were also done adding in I-405 traffic count data from the PeMS station approximately 450 m east of the CN site. As data were available only hourly, it cut the sample sizes by approximately half. However, results showed arrivals (positively) and wind speed (negatively) to be significantly correlated with UFP concentrations when the CE site was downwind of airport operations.

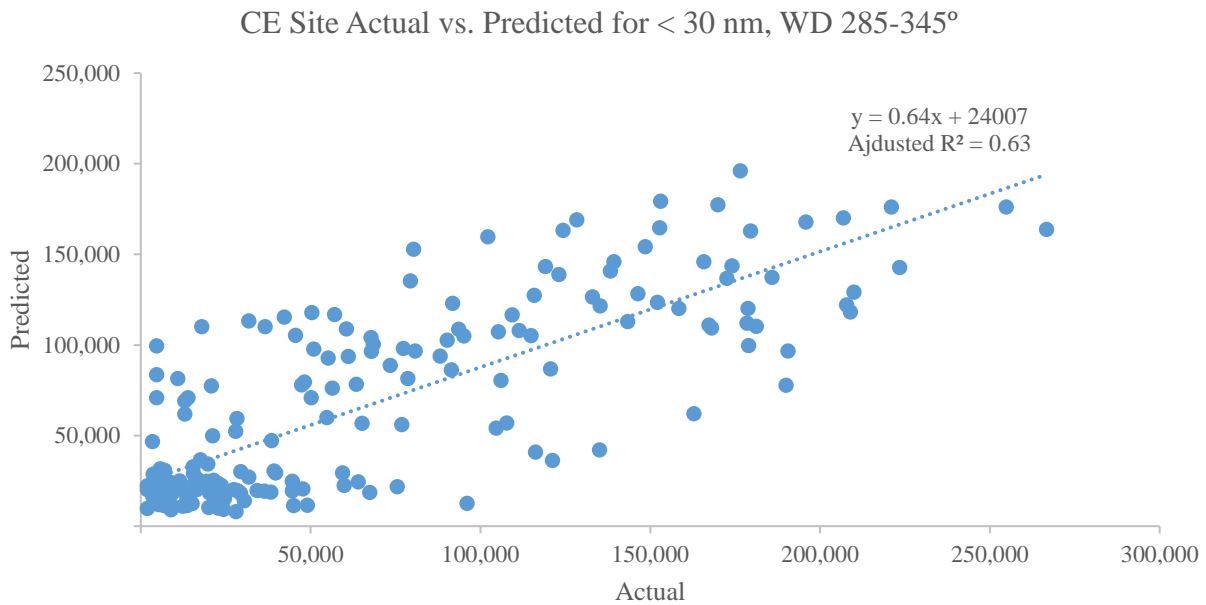


Figure 6. Actual versus predicted UFP concentration (< 30 nm) for multivariate regression results at the CE site for wind directions 285-345°.

Table 2 shows the regression coefficients, p-values, adjustment R<sup>2</sup>, and sample sizes for the CN site by 60° wind direction bin.

**Table 2: Regression Coefficients and p-values for CN Site UFP Concentrations < 30 nm**

CN SITE <30 NM Sample Size	ALL WD 868	225°-285° 600	285° -345° 62	45° -105° 30	105° -165° 69	165° -225° 101
<b>Constant</b>	9,390***	16,700***	-1,613	11,500***	9,840**	2,840
<b>coeff.</b>						
<b>p-value</b>	(0.00)	(0.00)	(0.85)	(0.00)	(0.01)	(0.70)
<b>RW24 (N) Arrival</b>	500	258	2,524***	890*	614	-330
	(0.06)	(0.42)	(0.00)	(0.02)	(0.12)	(0.65)
<b>RW24 (N) Departure</b>	368	530			65.9	607
	(0.11)	(0.06)			(0.87)	(0.38)
<b>RW25 (S) Arrival</b>	1,150***	1,150***				1,810**
	(0.00)	(0.00)				(0.01)
<b>RW25 (S) Departure</b>	-92.8	-13.2	143	37.8	263	-313
	(0.66)	(0.97)	(0.77)	(0.88)	(0.38)	(0.54)
<b>Wind Speed</b>	1,230	-835	5,435	-5,420**	-3,200	10,700*
	(0.11)	(0.43)	(0.31)	(0.01)	(0.26)	(0.02)
<b>Adjusted R<sup>2</sup></b>	0.18	0.07	0.38	0.27	0.06	0.31

\*p<0.05, \*\*p<0.01, \*\*\*p<0.001

Arrivals are also the most important predictors at the CN site for all wind directions with the exception of winds from the east, which as for the CE site, also show no impact from the airport. Operations on RW25 (S) are the most significant predictor of UFP at the CN site for winds from the west and southeast, when the CN site is downwind of operations on RW25 (S) (for winds from the west). Arrivals on RW24 (N) are significant contributors when winds are from the north and northwest, as for the CE site. Wind speed is also negatively correlated for winds from the east but positively correlated for the southerly winds.

UFP concentrations measured for winds from the northwest (Fig 7) had the highest adjusted R<sup>2</sup> value and provided the best fit, with the expressions (all variables significant).

$$\text{Predicted UFP} = -1,613 + 2,524 \text{ RW24 A (N)}$$

RW24 (N) arrivals was the only significant variable in the regression for the northwest wind direction. Plots for additional wind directions of actual versus predicted < 30 nm UFP concentrations can be found in the Appendix.

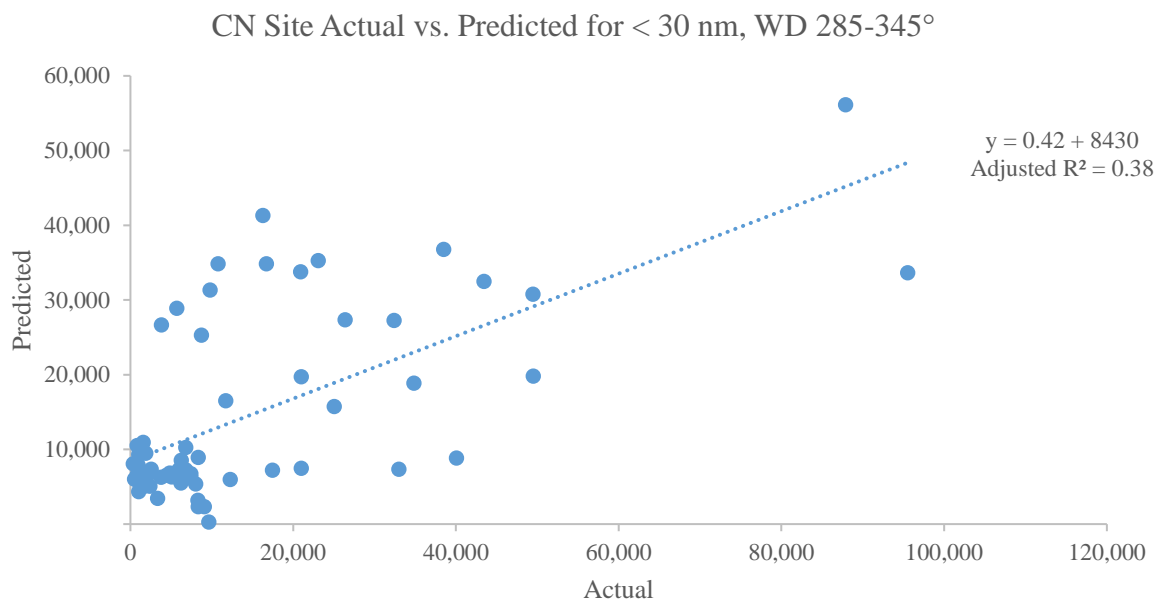


Figure 7. Actual versus predicted UFP concentration (< 30 nm) for multivariate regression results at the CN site for wind directions 285-345°.

Again, regressions were also done for the CN site adding in I-405 traffic count data from the PeMS station. Sample sizes for all wind directions, with the exception of 225-285°, were less than 50. However, results showed arrivals to be positively correlated with UFP concentrations when the CN site was downwind of airport operations or downwind of operations on South Airfield runways (southwest of the monitoring site).

#### 4. Discussion

Collection of size resolved UFP data during the LAX AQSAS was far from ideal; three-minute time resolution is too low to capture transient events associated with aircraft operations. However, some analyses are still possible.



Multiple lines of evidence indicate aircraft landing operations are the primary contributor to UFP concentrations < 30 nm at two sites between 1,600 and 2,000 m downwind of LAX. Sub-30 nm UFP are highly elevated when the sites are downwind of arrival operations on one or both RWs, directions that include fairly wide swaths of approximately 190-310°. Peak concentrations are observed at wind directions shifted from directly downwind from the nearest respective runway. Diurnal trends also show the influence of aircraft operations with UFP concentrations are consistent with a combination of wind direction, numbers of arriving flights, and wind speed, all of which vary (but which are usually fairly consistent from day to day) over the course of the day. Of the aircraft operation influence at the two sites, UFP concentrations < 30 nm are found to be primarily from arrivals on both the North and South Airfield runways 24/25. For the multivariate linear regression results, arrivals were significant when the two sites were downwind of the airport while departures were not.

Multiple studies consistently show that during the daytime, freeway plumes are typically > 90 percent dissipated in 100 m disappear completely in 300 m (Karner et al., 2010). Plumes can persist for much longer distances in a stable nocturnal surface layer, up to 2,500 m (Hu et al., 2009b; Choi et al., 2013), but at LAX when a nocturnal surface layer develops, it is associated with winds from the N/NE, wind directions that are not associated with elevated < 30 nm UFP from aircraft operations. Aircraft takeoff operations have much higher concentrations of UFP than are typically observed around roadways (Westerdahl et al., 2008; Hu et al., 2009a, Keuken et al., 2015), thus takeoff plumes might be expected further downwind than freeway plumes. Zhu et al. (2011) were able to assign individual peaks to aircraft departures at LAX 600 m downwind. However, there is no evidence in the literature directly associating elevated concentrations 1,600 – 2,000 m with takeoff events.

The sites where SMPS data were collected for the LAX AQSAS are located almost 2 km downwind from the end of the North and South Airfield runways. To gain a better understanding of the contribution of both arrivals and departures, multiple tandem sites should be set up to collect measurements from the end of the runways or behind the blast fence as well as directly under the arrivals path. This can help to determine at which point UFP concentrations are dominated by one operational type over another, if at all. SMPS measurements were taken on a three-minute time resolution for the LAX AQSAS making it impossible to assign a specific peak value to a specific operation. It also does not allow for specifically distinguishing between arrivals versus departures. Measurements should be taken on a faster time resolution of, at the very least, one minute.

## **Appendix**

### *Introduction*

Zhu et al. (2011) measured particle size distributions from aircraft operations at the blast fence and found the highest numbers to be a particle size of 14 nm for takeoff operations at LAX (Zhu et al., 2011). Westerdahl et al. (2008) found a downwind site 100 m from LAX to be dominated by particles between 10-15 nm while particles at an upwind site were dominated by 90 nm particles. At Schiphol Airport in the Netherlands, Keuken et al. (2015) measured particle number concentrations that were dominated by UFP ranging from 10-20 nm. At Santa Monica Airport, a small general aviation airport, the median size mode of UFP measured from aircraft was 11 nm (Hu et al., 2009a). Lobo et al. (2012) determined the geometric mean diameter for aircraft takeoff emissions measured 300 m downwind of the Oakland Airport to be  $13.2 \pm 5.3$  nm.

### *Methods*

#### UFP Measurements

Scanning Mobility Particle Sizers (SMPS) operated at the CE and CN sites for the full season and took continuous measurements of particle size distributions. Desert Research Institute provided the instruments which included an SMPS 3936N25A (TSI Inc., Shoreview, MN) and SMPS 3936L10 (TSI Inc., Shoreview, MN) at the CN and CE sites, respectively. The Grimm SMPS+C (Grimm Aerosol Technik, Ainring, Germany) originally operated at the CE Site but was moved at the beginning of the Summer Season. The TSI replaced the Grimm at the CE site for the remainder of the Summer Season. NaCl particle size distribution was measured in the DRI laboratory by the three collocated SMPS.

The SMPS system consisted of three components including a bipolar charger, mobility classifier, and condensation particle counter (CPC). The two instruments had the capability of

measuring distributions in the range of 2.5 to 150 nm (3936N25A) and 5.4 to 358 nm (3936L10). The range of particle sizes measured at the CE site was 5.5 to 289 nm and for the CN site was 4.6 to 156 nm. The CE and CN sites SMPS's collected particle counts by size bin (dN/dlogDp), mass ( $\mu\text{g m}^{-3}$ ), volume ( $\text{um}^3 \text{cc}^{-1}$ ), and the concentration of the predetermined particles sizes ( $\# \text{cm}^{-3}$ ) including total concentration, 5.5-30, and 30-156 nm. The SMPS used was on 64 channel resolution. The provided data were in terms of dN/dlogDp for both instruments (TSI, 2010). To determine the raw concentrations, each bin multiplied by dlogDp (TSI, 2010) and summed for the designated sizes (< 30 and 30-98 nm). This was checked by comparing calculated concentrations with those provided in the SMPS data set.

### Results

**Table A1: Operations by Runway**

<b>RUNWAY</b>	<b>ARRIVALS</b>	<b>DEPARTURES</b>	<b>TOTAL</b>
<b>25R/L</b>	19,296	20,601	39,897
<b>24R/L</b>	15,462	12,891	28,353
<b>06R/L</b>	1,142	17	1,159
<b>07R/L</b>	379	4	383
<b>TOTAL</b>	36,279	33,513	69,792

Table A1 includes total operational counts for arrivals and departures by runway. There is a difference between arrivals and departures during the Summer Season. There were 2,766 more arrivals than departures recorded. The largest differences between arrivals and departures were for the larger airlines: American Airlines (469 more arrivals), Southwest (375), Delta (339), United (249), Skywest (198), Alaska (149), American Eagle (143), Virgin (106), and US Airways (103).

### Results

Figs. A1 through A8 includes plots of Actual versus Predicted UFP values for CE and CN Site for each designated wind bin.

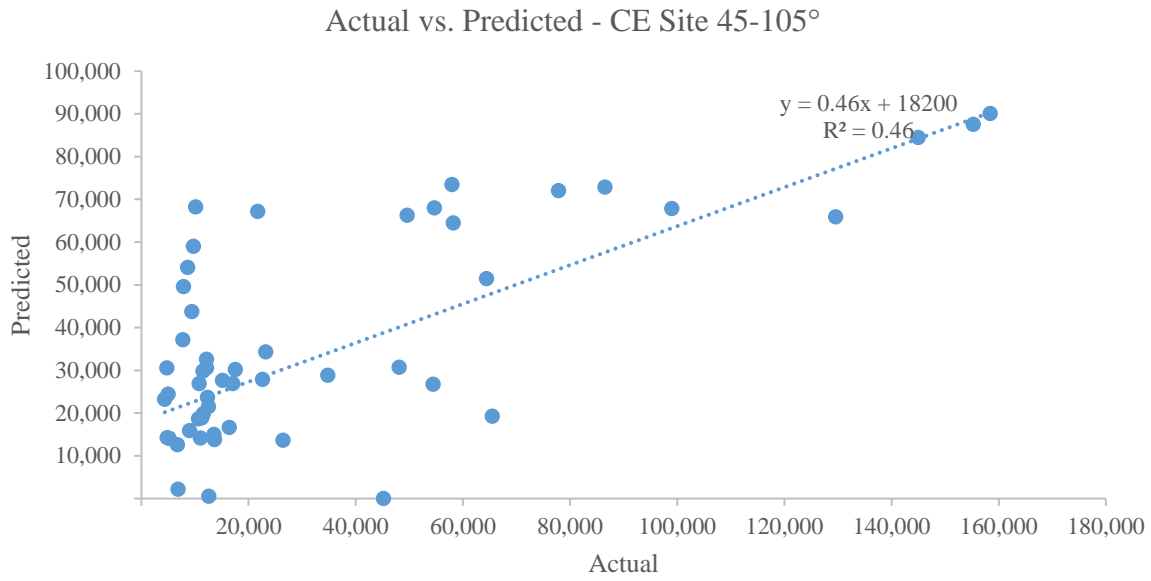


Figure A1. Actual versus predicted UFP concentration (< 30 nm) for multivariate regression results at the CE site for wind directions 45-105°.

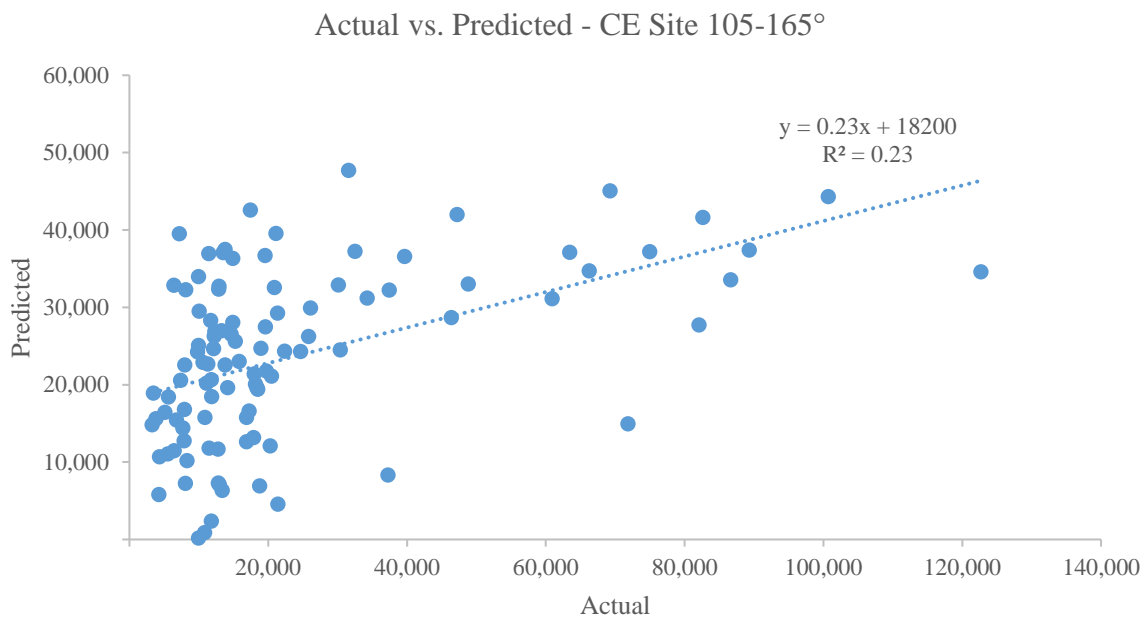


Figure A2. Actual versus predicted UFP concentration (< 30 nm) for multivariate regression results at the CE site for wind directions 105-165°.

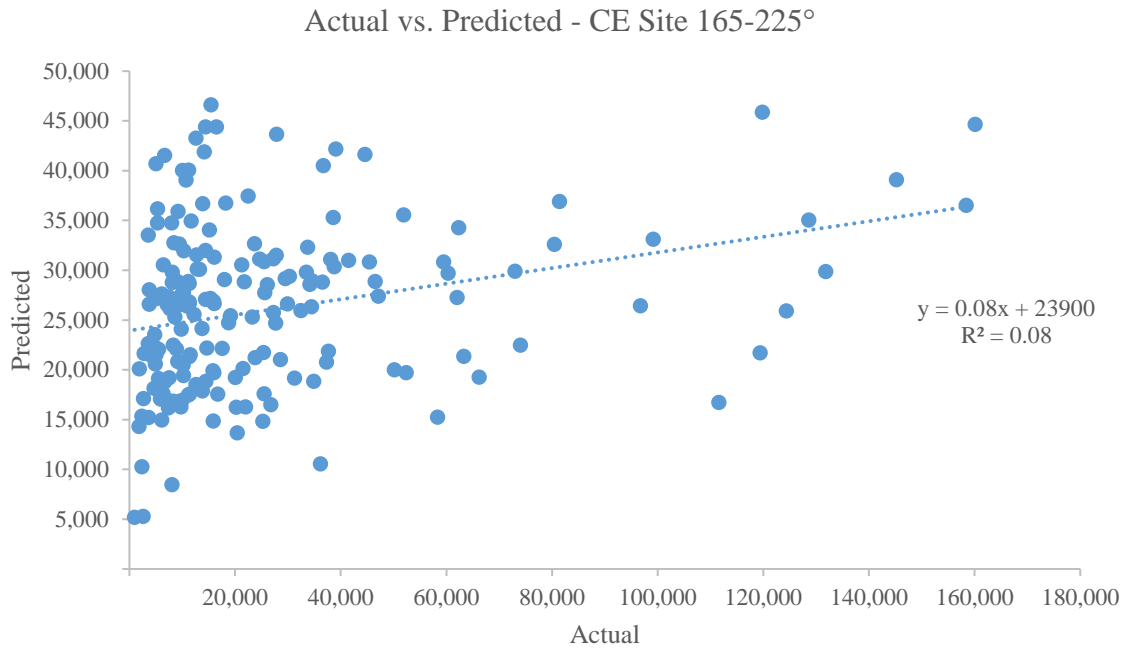


Figure A3. Actual versus predicted UFP concentration (< 30 nm) for multivariate regression results at the CE site for wind directions 165-225°.

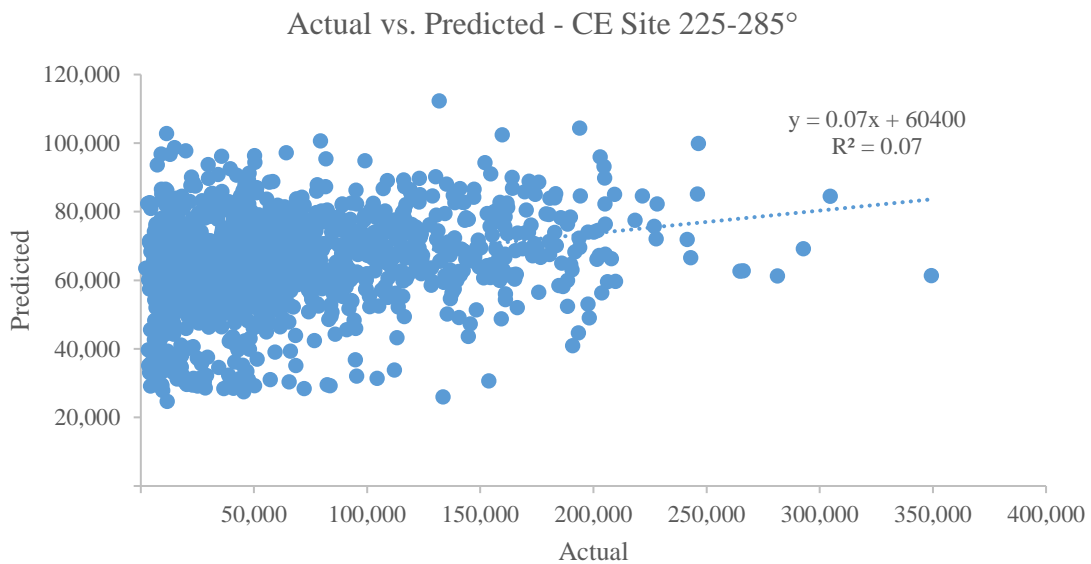


Figure A4. Actual versus predicted UFP concentration (< 30 nm) for multivariate regression results at the CE site for wind directions 225-285°.

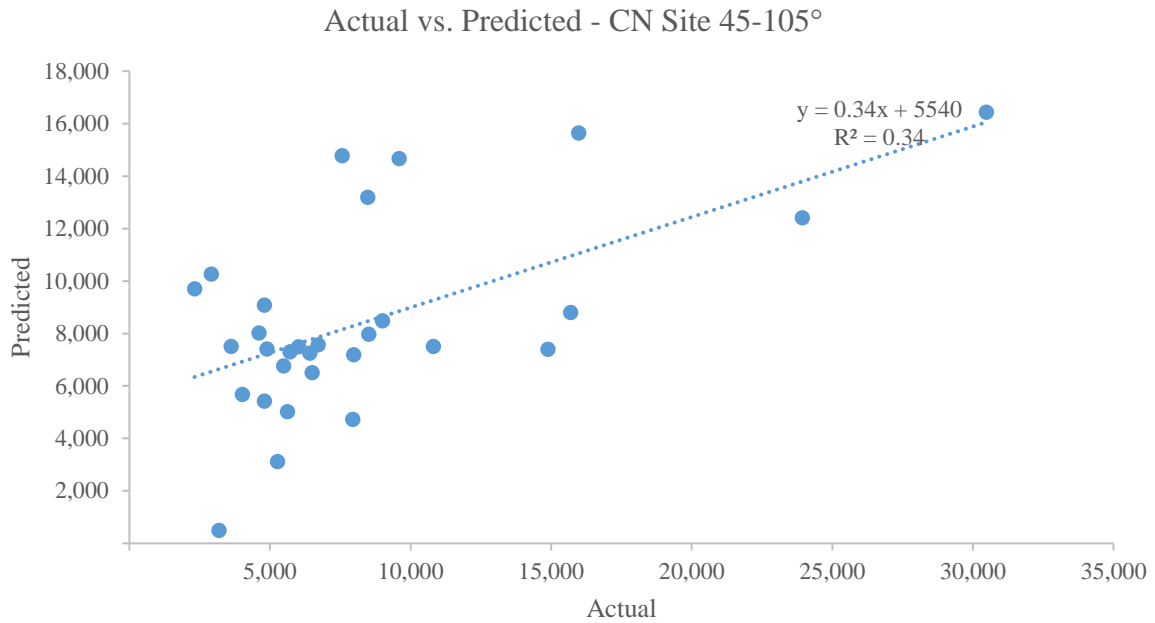


Figure A5. Actual versus predicted UFP concentration (< 30 nm) for multivariate regression results at the CN site for wind directions 45-105°.

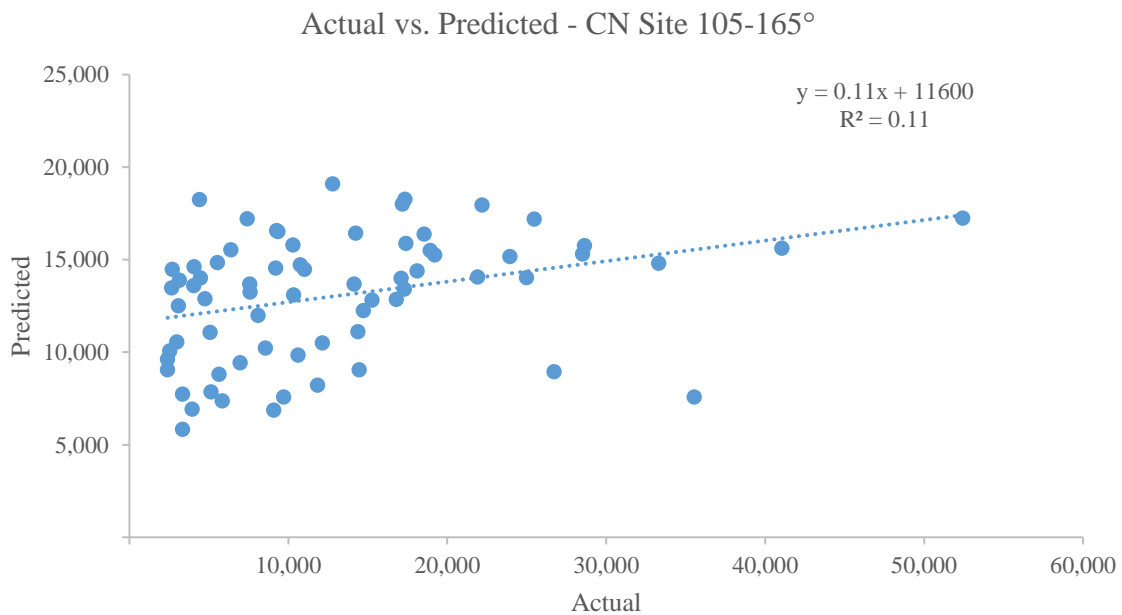


Figure A6. Actual versus predicted UFP concentration (< 30 nm) for multivariate regression results at the CN site for wind directions 105-165°.

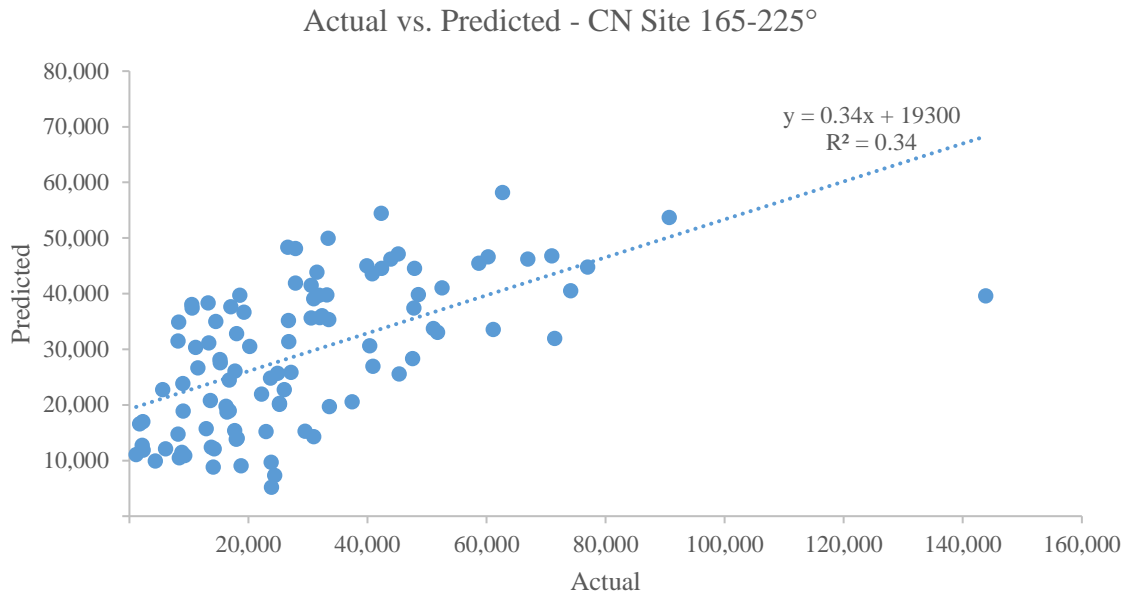


Figure A7. Actual versus predicted UFP concentration (< 30 nm) for multivariate regression results at the CN site for wind directions 165-225°.

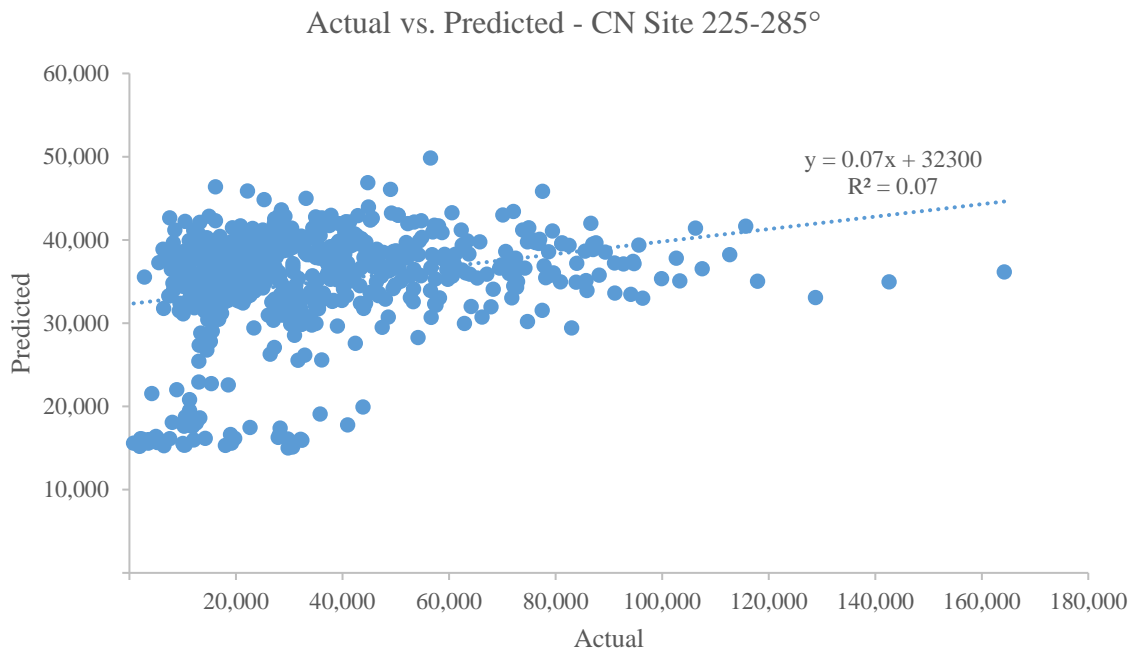


Figure A8. Actual versus predicted UFP concentration (< 30 nm) for multivariate regression results at the CN site for wind directions 225-285°.



## References

- Atmospheric Science Data Center (distributor). 2003. Dry-Ambient Size Spectrometer (Non-SMPS, SMPS, APS) Data Quality Statement. Pittsburgh Air Quality Study July 1, 2001-June 30, 2002. Accessed from: [https://eosweb.larc.nasa.gov/sites/default/files/project/narsto/guide/DAASS\\_Data\\_Qual\\_Statement.pdf](https://eosweb.larc.nasa.gov/sites/default/files/project/narsto/guide/DAASS_Data_Qual_Statement.pdf)
- California Department of Transportation. 2018. Performance Measurement System (PeMS) Data Source. <http://pems.dot.ca.gov/>
- Carslaw DC, Beevers SD, Ropkins K, and MC Bell. 2006. Detecting and quantifying the contribution made by aircraft emissions to ambient concentrations of nitrogen oxides in the vicinity of a large international airport. *Atmospheric Environment*. 40(28): 5424-5434.
- Chalupa DC, Morrow PE, Oberdorster G, Utell MJ, and MW Frampton. 2004. Ultrafine deposition in subjects with asthma. *Environ Health Perspect*. 112(8): 879-882.
- Choi, W., D. Ranasinghe, K. Bunavage, J.R. DeShazo, L. Wu, R. Seguel, A.M. Winer, and S.E. Paulson. 2016. The effects of the built environment, traffic patterns, and micrometeorology on street level ultrafine particle concentrations at a block scale: Results from multiple urban sites. *Sci. Tot. Environ*. 15;553:474-85. doi: 10.1016/j.scitotenv.2016.02.083.
- Choi W, Hu Shishan, He Meilu, Kozawa K, Mara S, Winer AM, and SE Paulson. 2013. Neighborhood-scale air quality impacts of emissions from motor vehicles and aircraft. *Atmos Environ*. 80: 310-321.

- Choi W, He M, Barbesane V, Kozawa KH, Mara S, Winer AM, and SE Paulson. 2012. Prevalence of wide area impacts downwind of freeways under pre-sunrise stable atmospheric conditions. *Atmos Environ.* 62: 318-327.
- Chow JC, Watson JG, Doraiswamy P, Chen LWA, Sodeman DA, Hang Ho SS, Kohl SD, Trimble DL, and H Voepel. 2006. Climate Change – Characterization of Black Carbon and Organic Carbon Air Pollution Emissions and Evaluation of Measurement Methods. Prepared for California Air Resources Board and California Environmental Protection Agency.
- Delfino RJ, Sioutas C, and S Malik. 2005. Potential Role of Ultrafine Particles in Associations between Airborne Particle Mass and Cardiovascular Health. *Environ Health Perspect.* 113(8); 934-946.
- Dodson RE, Houseman EA, Morin B, and JI Levy. 2009. An Analysis of Continuous Black Carbon Concentrations in Proximity to an Airport and Major Roadways. *Atmospheric Environment.*
- Gong Jr. H, Linn WS, Clark KW, Anderson KR, Sioutas C, Alexis NE, Cascio WE, and RB Devlin. 2008. Exposures of Healthy and Asthmatic Volunteers to Concentrated Ambient Ultrafine Particles in Los Angeles. *Inhalation Toxicology.* 20(6): 533-545.
- Herndon SC, Onasch TB, Frank BP, Marr LC, Jayne JT, Canagaratna MR, Grygas J, Lanni T, Anderson BE, Worsnop D, and RC Mlake-Lye. 2005. Particulate Emissions from in-use Commercial Aircraft. *Aerosol Science and Technology.* 39(8): 799-809.
- Hoek G, Boogaard H, Knol A, De Hartog J, Slottje P, Ayres JG, Borm P, Brunekreef B, Donaldson K, Forastiere F, Holgate S, Kreyling WG, Nemery B, Pekkanen J, Stone V, Wichmann HE, and J Van Der Sliujs. 2010. Concentration response functions for ultrafine particles and

- all-cause mortality and hospital admissions: Results of a European expert panel elicitation. *Environ. Sci and Technol.* 44(1): 476-482.
- Hsu HH, Adamkiewicz G, Houseman EA, Spengler JD, and JI Levy. 2014. Using mobile monitoring to characterize roadway and aircraft contributions to ultrafine particle concentrations near a mid-sized airport. *Atmospheric Environment.* 89: 688-695.
- Hsu HH, Adamkiewicz G, Houseman EA, Zarubiak D, Spengler JD, and JI Levy. 2013. Contributions of aircraft arrivals and departures to ultrafine particle counts near Los Angeles International Airport. *Science of the Total Environment.* 444. 347-355.
- Hsu HH, Adamkiewicz G, Houseman EA, Vallarino J, Melly SJ, Wayson RL, Spengler JD, and JI Levy. 2012. The relationship between aviation activities and ultrafine particulate matter concentrations near a mid-sized airport. *Atmospheric Environment.* 50: 328-337.
- Hu S, Fruin S, Kozawa K, Mara S, Winer AM, and SE Paulson. 2009a. Aircraft Emission Impacts in a Neighborhood Adjacent to a General Aviation Airport in Southern California. *Environ. Sci. Technol.* 43. 8039-8045.
- Hu S, Fruin S, Kozawa K, Mara S, Paulson SE, and AM Winer. 2009b. A Wide Area of Air Pollutant Impact Downwind of a Freeway during Pre-Sunrise Hours. *Atmos Environ.* 43(16): 2541-2549.
- Hudda N and SA Fruin. 2016. International Airport Impacts to Air Quality: Size and Related Properties of Large Increases in Ultrafine Particle Number. *Environ. Sci. Technol.* 50. 3362-3370.
- Hudda N, Gould T, Hartin K, Larson TV, and S Fruin. 2014. Emissions from an International Airport Increase Particle Number Concentrations 4-fold at 10 km downwind. *Environ. Sci. Technol.* 48. 6628-6635.

- Karner AA, Eisinger DS, and DA Niemeier. 2010. Near-Roadway Air Quality: Synthesizing the Findings from Real-World Data. *Environ. Sci. & Technol.* 44: 5334-5344.
- Keuken MP, Moerman M, Zandveld P, Henzing JS, and G Hoek. 2015. Total and size-resolved particle number and black carbon concentrations in urban areas near Schiphol airport (the Netherlands). *Atmospheric Environment.* 104: 132-142.
- Lobo P, Hagen DE, and PD Whitefield. 2012. Measurements and analysis of aircraft engine PM emissions downwind of an active runway at the Oakland International Airport. *Atmospheric Environment.* 61: 114-123.
- Los Angeles International Airport. 2018. Efforts to Reduce or Limit Aircraft Noise at LAX. Accessed from: <https://www.lawa.org/en/lawa-environment/noise-management/lawa-noise-management-lax/efforts-to-reduce-or-limit-aircraft-noise-at-lax>
- Los Angeles World Airports. 2013. LAX Air Quality and Source Apportionment Study. Volume 2 – Phase III. Accessed from: <https://www.lawa.org/-/media/lawa-web/environment/files/vol-2---lax-aqsas-2014-03-11s.ashx?la=en&hash=64E3AFD29F56BB75744405E6F40192BAC261FDB0>
- Moore RH, Shook MA, Ziemba LD, DiGangi JP, Winstead EL, Rauch B, Jurkat T, Thornhill KL, Crosbie EC, Robinson C, Shingler TJ, and BE Anderson. 2017. Take-off engine particle emission indices for in-service aircraft at Los Angeles International Airport. *Scientific Data.* 4: 170198 doi: 10.1038/sdata.2017.198 (198)
- Morawska L, Bofinger ND, Kocis L, and A Nwankwoala. 1998. Submicrometer and super micrometer particles from diesel vehicle emissions. *Environ. Sci. Technol.* 32: 2033-2042.
- Oberdorster G. 2000. Pulmonary effects of inhaled ultrafine particles. *International Archives of Occupational and Environmental Health.* 74(1): 1-8.

- Park K, Chow JC, Watson JG, Trimble DL, and P Doraiswamy. 2006. Comparison of Continuous and Filter-Based Carbon Measurements at the Fresno Supersite. *J. Air & Waste Manage. Assoc.* 56:474-491.
- Penttinen P, Timonen KL, Tittanen P, Mirme A, Ruuskanen J, and J Pekkanen. 2001. Ultrafine particles in urban air and respiratory health among adult asthmatics. *European Respiratory Journal.* 17: 428-435.
- Peters A, Wichmann HE, Tuch T, Heinrich H, and J Heyder. 1997. Respiratory Effects Are Associated with the Number of Ultrafine Particles. *Am J Respir Crit Care Med.* 155: 1376-1383.
- Pietropaoli AP, Frampton MW, Hyde RW, Morrow PE, Oberdorster G, Cox C, Speers DM, Frasier LM, Chalupa DC, Huang L, and MJ Utell. 2004. Pulmonary Function, Diffusing Capacity, and Inflammation in Healthy and Asthmatic Subjects Exposure to Ultrafine Particles. *Inhal. Toxicol. Sup 1:* 59-72.
- Riley EA, Gould T, Hartin K, Fruin SA, Simpson CD, Yost MG, and T Larson. 2016. Ultrafine particle size as a tracer for aircraft turbine emissions. *Atmos Environ.* 139: 20-29. Doi: 10.1016/j.atmosenv.2016.05.016
- Ristovski ZD, Morawska L, Bofinger ND, and J Hitchins. 1998. Submicrometer and supermicrometer particles from spark ignition vehicles. *Environ. Sci. Technol.* 32: 3845-3852.
- TSI. 2010. Aerosol Statistics. Lognormal Distributions and  $dN/d\log D_p$ . Application Note PR-001. Accessed from: [http://www.tsi.com/uploadedFiles/Product\\_Information/Literature/Application\\_Notes/PR-001-RevA\\_Aerosol-Statistics-AppNote.pdf](http://www.tsi.com/uploadedFiles/Product_Information/Literature/Application_Notes/PR-001-RevA_Aerosol-Statistics-AppNote.pdf)

- Unal A, Hu Y, Change ME, Odman MT, and AG Russell. 2005. Airport related emissions and impacts on air quality: Application to the Atlanta International Airport. *Atmospheric Environment*. 39: 5787-5798.
- Westerdahl D, Fruin SA, Fine PL, and Sioutas C. 2008. The Los Angeles International Airport as a source of ultrafine particles and other pollutants to nearby communities. *Atmospheric Environment*. 42: 3143-3155
- Zhu Y, Fanning E, Yu RC, Zhang Q, and JR Froines. 2011. Aircraft emissions and local air quality impacts from takeoff activities at a large International Airport. *Atmospheric Environment*. 45: 6526-6533.

## Conclusion

Aircraft operations, including takeoff and landing, contribute to ultrafine particles (UFP) concentrations downwind of airports such as Santa Monica Airport and Los Angeles International Airport (SMO and LAX). Use of other parameters, including wind direction, wind speed, aircraft operation, and emission rates from the International Civil Aviation Organization (ICAO) database, to further determine UFP concentrations downwind of airports are beneficial.

### *Santa Monica Airport (SMO)*

UFP data analyzed for SMO was able to be assigned to peak concentrations for both takeoff and landing operations with takeoff UFP concentrations significantly higher than landing. Plots of  $\pm 5$  minutes from an operation showed clearly defined peaks, which rapidly dropped reaching background concentrations soon after takeoff or landing. While the ability to assign specific peaks to takeoff operations agrees with findings from other studies (Unal et al., 2005; Westerdahl et al., 2008; Hu et al., 2009; Zhu et al., 2011; Hsu et al., 2013; Hudda et al., 2014; Moore et al., 2017), few studies assign specific peaks to specific landing operations. For this analyses, we were able to assign UFP peak concentrations to specific landing operations at SMO.

Aircraft operate at higher thrust during takeoff and climbout and lower thrust during approach and idle. At the Residential Site (Ernst Site) located 100 m from the end of the SMO runway, UFP concentrations from takeoff operations were 60 percent higher than landings. Multiple studies have reported higher emission rates for higher thrust and increased engine power (Agrawal et al., 2008; Wey et al., 2006; 2007; Mazaheri et al., 2009; Lobo et al., 2012).

Using single variable linear regression for each ICAO parameters (oxides of nitrogen [NO<sub>x</sub>], hydrocarbons [HCs], carbon monoxide [CO], and smoke number [SN]), we identified important ICAO parameters in predicting UFP concentrations. Overall, thrust (kN) was the most significant

predictor of UFP concentrations for takeoff operations. NO<sub>x</sub> emission rates are also an important predictor of UFP concentrations. Additionally, NO<sub>x</sub> and thrust are strongly correlated, which supports the use of thrust and NO<sub>x</sub> as the strongest predictors of UFP. No ICAO parameters for the single variable linear regression were significant in predicting UFP concentrations from landing operations.

An analysis of correlations between ICAO parameters showed NO<sub>x</sub> and thrust to be highly correlated for all components of the landing takeoff (LTO) cycle. The data for the remaining variables were smaller, therefore, it was not possible to reach a significant conclusion.

The use of engine age in determining UFP concentrations found no significant difference exists between older and newer vintages engines for takeoff, landing, or combined takeoff and landing operations. Additionally, when UFP peak concentrations were normalized by thrust, no significant difference was observed as well.

#### *Los Angeles International Airport (LAX)*

Data from the LAX Air Quality and Source Apportionment Study, including particle concentrations, wind direction, wind speed, time of day, and aircraft were used to determine the impact of UFP concentrations at two community sites between 1,600 and 2,000 meters (m) downwind of LAX. When the two sites (Community East [CE] and Community North [CN]) were downwind of the airport, the UFP measurements were dominated by particles < 30 nm. The concentrations of particles < 30 nm were determined to have large contributions from aircraft arrival operations but not from departures or nearby roadways.

Sub-30 nm UFP were predominantly from arrival operations and meteorology. The CE and CN sites exhibited patterns of the highest < 30 nm concentrations when downwind from the airport and the lowest when upwind of the airport. At the CE site, concentrations were highest for winds



from the northwest, indicating influence from arrivals. At the CN site, concentrations were highest again for winds from the northwest, as well as the southwest. This indicates the influence of landing operations on the North Airfield runways (24R/L), which pass directly over the monitoring site, as well as contributions from landing operations on the South Airfield where arrivals touchdown to the southwest of the monitoring site. The pattern for 30-98 nm particles showed less diurnal variation and no discernable peaks when the two sites were downwind of the airport. Average concentrations for the 30-98 nm particles varied slightly while < 30 nm concentrations varied much more widely. The < 30 nm UFP was nearly 2 times higher at the CE vs. CN site while the 30-98 nm particles were only slightly higher at the CN site.

A multivariate linear regression of arrivals and departures on RW24 (North [N]) and 25 (South [S]) found arrivals to be significant contributors to the UFP concentrations measured at the two sites during wind directions when the sites were downwind of the airport. Regression results at the CE site are strongest for winds from the northwest, which capture operations from the North Airfield as well as the end of RW25 R (S) which was located at approximately 280°. When traffic data from a PeMS I-405 freeway station were added to the regression, sample sizes were much smaller; however, arrivals were still correlated with UFP concentrations.

### *Summary*

UFP concentrations are able to be attributed to aircraft operations from both SMO, a small general aviation airport, and LAX, a large international airport. Peaks can be assigned to both takeoff and landing operations at two sites downwind of SMO located 35 and 100 m downwind of the end of the runways. ICAO database parameters, including thrust and NO<sub>x</sub> are useful in predicting UFP concentrations.

Sub-30 nm UFP measurements during the LAX Air Quality and Source Apportionment Study can be attributed to aircraft arrival operations at LAX. Additionally, when the two sites were downwind of the airport, the highest < 30 nm particles were measured. At the two sites used here, UFP concentrations result primarily from arrival operations with no influence from departures observed. The sites were located between 1,600 and 2,000 meters, which could be at too great a distance to observe influence from departures.

## References

- Agrawal H, Sawant AA, Jansen K, Wayne Miller, J., Cocker III, D.R., 2008. Characterization of chemical and particulate emissions from aircraft engines. *Atmospheric Environment* 42, 4380-4392.
- Hsu HH, Adamkiewicz G, Houseman EA, Zarubiak D, Spengler JD, and JI Levy. 2013. Contributions of aircraft arrivals and departures to ultrafine particle counts near Los Angeles International Airport. *Science of the Total Environment*. 444. 347-355.
- Hu S, Fruin S, Kozawa K, Mara S, Paulson SE, and AM Winer. 2009. A Wide Area of Air Pollutant Impact Downwind of a Freeway during Pre-Sunrise Hours. *Atmos Environ*. 43(16): 2541-2549.
- Hudda N, Gould T, Hartin K, Larson TV, and S Fruin. 2014. Emissions from an International Airport Increase Particle Number Concentrations 4-fold at 10 km downwind. *Environ. Sci. Technol*. 48. 6628-6635.
- Lobo P, Hagen DE, and PD Whitefield. 2012. Measurements and analysis of aircraft engine PM emissions downwind of an active runway at the Oakland International Airport. *Atmospheric Environment*. 61: 114-123.
- Mazaheri M, Johnson GR, and L Morakawa. 2009. Particle and Gaseous Emissions from Commercial Aircraft at Each Stage of the Landing and Takeoff Cycle. *Environ. Sci. Technol*. 43. 441-446.
- Moore RH, Shook MA, Ziemba LD, DiGangi JP, Winstead EL, Rauch B, Jurkat T, Thornhill KL, Crosbie EC, Robinson C, Shingler TJ, and BE Anderson. 2017. Take-off engine particle emission indices for in-service aircraft at Los Angeles International Airport. *Scientific Data*. 4: 170198 doi: 10.1038/sdata.2017.198 (198)

- Westerdahl D, Fruin SA, Fine PL, and Sioutas C. 2008. The Los Angeles International Airport as a source of ultrafine particles and other pollutants to nearby communities. *Atmospheric Environment*. 42: 3143-3155.
- Wey, C.C., Anderson, B.E., Hudgins, C., Wey, C., Li-Jones, X., Winstead, E., Thornhill, L.K., Lobo, P., Hagen, D., Whitefield, P., Yelvington, P.E., Herndon, S.C., Onasch, T.B., Miake-Lye, R.C., Wormhoudt, J., Knighton, W.B., Howard, R., Bryant, D., Corporan, E., Moses, C., Holve, D., Dodds, W., 2006. Aircraft Particle Emissions Experiment (APEX). NASA/TM-2006e214382, ARL-TR-3903. U.S. National Aeronautics and Space Administration, Glenn Research Center, Cleveland, OH. Available at: <http://gltrs.grc.nasa.gov>.
- Wey, C.C., Anderson, B.E., Wey, C., Miake-Lye, R.C., Whitefield, P., Howard, R., 2007. Overview on the aircraft particle emissions Experiment. *Journal of Propulsion and Power* 23, 898e905.
- Unal A, Hu Y, Change ME, Odman MT, and AG Russell. 2005. Airport related emissions and impacts on air quality: Application to the Atlanta International Airport. *Atmospheric Environment*. 39: 5787-5798.